Geoscience BC

Report 2015-02

Investigation of Tree Sap as a Sample Medium for Regional Geochemical Exploration in Glacial Sediment Covered Terrains: A Case History from the Endako area, North-Central BC (NTS map sheets 093F14, 093F15, 093K03 and 093K02)

David R. Heberlein
Colin E. Dunn
Eric Hoffman

Heberlein Geoconsulting
Extracting value from geochemistry

Actlabs
Quality Analysis... Innovative Technologies

Investigation of Tree Sap as a Sample Medium for Regional Geochemical Exploration in Glacial Sediment Covered Terrains: A Case History from the Endako area, North-Central BC (NTS map sheets 093F14, 093F15, 093K03 and 093K02)

Geoscience BC Report 2015-02

Spruce sap on bark of tree trunk and collection obtained for analysis

By

David R. Heberlein[1], Colin E. Dunn[2] and Eric Hoffman[3]

[1] Heberlein Geoconsulting, Suite 303-108 West Esplanade. North Vancouver, BC, V7M 3M8

[2] Colin Dunn Consulting Inc., 8756 Pender Park Drive, North Saanich, BC, V8L 3Z5

[3]Activation Laboratories Ltd., 41 Bittern Street, Ancaster, ON, L9G4V5

EXECUTIVE SUMMARY

This work was undertaken to determine if tree sap could provide a useful and possibly unique geochemical signal to buried mineralization. Congealed sap samples were collected in two sampling campaigns (September 2013 and May 2014) from the surfaces of more than 100 white spruce trees from over an area of 1000 km^2 surrounding the Endako Mo mine. For comparison, soil pH measurements were made, and Ah soils were collected at the same locations. Lodgepole pine sap was also obtained from a few sites in order to compare the spruce sap chemistry with that of pine. An additional database of element concentrations in pine bark collected in the 1990s from the same general area also was available for comparison. Work by others in Finland and Siberia, as well as a recent Geoscience BC survey over the Woodjam Cu porphyry deposit, demonstrated a strong positive response of both commodity and pathfinder elements in spruce sap over blind or buried mineralization. Whereas previous analytical work was undertaken at research institutes, a new generation high-sensitivity ICP-MS is now available commercially, allowing method development to determine ultra-low (sub-ppb) concentrations of a wide range of elements at modest cost.

A sampling strategy was developed to efficiently collect clean sap samples, which are critical to the process. The samples were sent to Actlabs, Ancaster, for analytical method development. After experimenting with many digestion methods, it was concluded that the optimal method involved initial dissolution of the sap in methanol followed by 0.45 µm filtration to remove contaminants. Filtered sap was then allowed to dry and the reconstituted material was re-dissolved in nitric-perchloric acid. Analysis was carried out by an Agilent 7700 ICP-MS, This instrument minimizes normal ICP-MS interferences from oxides or chlorides using the dual gas/no gas modes.

Data from field duplicate sample pairs showed that for elements with concentration levels close to the detection limit the analytical precision was poor. However, for elements with concentrations well above detection levels precision was considerably improved and meaningful plots of the data could be made for some elements. This was especially true for the element of principal interest (Mo) and several pathfinder and major elements, including Re, Bi, U, REE, Th, K, Rb, P, Na, Mn, Cs, Ag and Sr. Consequently, this report focuses on these elements, most of which are highly anomalous at sites around the mine over a surrounding area of approximately 50 km^2. Background to anomaly contrast was similar in saps, Ah horizon and pine bark. Sap samples from the vicinity of Mo mineralization near Nithi Mountain did not produce a discernible response for Mo, but anomalies for Bi and W were detected close to the known mineralization. It is concluded that sample spacing was perhaps too coarse to clearly define the small mineral occurrences.

A comparison of sap compositions from adjacent spruce and pine trees at 5 sample stations indicated similar concentrations of some elements, but consistent differences in others. It is concluded that the data from the two species could not be integrated or levelled without first obtaining much larger sample populations for comparison.

Comparisons of element distribution patterns in spruce sap, Ah horizon soils and a collection of pine bark samples collected 15 years ago showed that Mo, U, Th and REE displayed broadly similar patterns in all media, but with slightly better defined signatures in the spruce sap. Tungsten in Ah and pine bark delineated the mine area well, but not as well in sap.

Soil pH readings from Ae or B horizon material collected at each sap sample location showed a robust H^+ response surround the Endako ore body and extending for distances of up to 1.2 km to the northwest, 3.4 km to the east and 1.6 km to the south. Highest values occur peripheral to a K radiometric anomaly that defines the extent of potassic alteration. The halo of high H^+ values is interpreted to indicate the extent of the pyrite halo around the margins of porphyry Mo system.

It is concluded that if appropriate sampling protocols are followed spruce sap is an effective sample medium for regional scale exploration for porphyry Mo mineralization and there seems no impediment to using this method with other styles mineralization. Spruce sap is easy to collect and can be submitted for analysis with no further preparation required. Element concentrations are mostly in the ppb range and so precision is likely to be inferior to that usually obtained from the analysis of soils or live vegetation. However in areas of suspected contamination the sap might be a preferred sample medium since it derives its chemical signature from deep in the ground. Furthermore the digestion procedure developed for this project further excludes potential dust contamination from the analytical sample. The congealed sap contains the geochemical signature of major elements that are surplus to the trees' metabolic function as well as pathfinder elements that perform no known function in plant growth and health, and so become readily exuded.

TABLE OF CONTENTS

Contents

LIST OF FIGURES

LIST OF TABLES

LIST OF APPENDICES

INTRODUCTION

Large areas prospective for porphyry and epithermal-style mineralization in central British Columbia are covered by Cenozoic basalt flows and or Quaternary glacial sediments. A recent Geoscience BC study carried out at Goldfield's Woodjam, BC, property (Bissig *et al.,* 2013; Heberlein *et al*., 2013) tested a variety of analytical methods on organic or organically-derived sample media aimed at establishing a geochemical strategy to detect blind porphyry Cu-Au mineralization through glacial deposits and Cenozoic basalts. Results revealed a good response of Cu in spruce sap, but equally importantly for exploration, a strong response in the pathfinder elements As, Hg and W. Metals taken up by tree roots, and of importance for metabolism, such as Cu, are sequestered in cells while excess amounts of non-essential and toxic elements are thought to be generally transported through the plant to be either transpired in some form (such as vapour or particulates) or exuded in sap, which commonly congeals as globules on the trunks of some tree species. Consequently, the analysis of commodity and toxic or non-essential 'pathfinder' elements in tree sap would provide a useful and potentially unique method for mineral exploration. Analytical technology using high-resolution ICP-MS or new generation high-sensitivity ICP-MS is now available commercially, and the development of methodology and 'proof of concept' derived from the prior year's detailed work for Geoscience BC can now be examined on a broader scale.

Tree sap is potentially useful for regional and local scale exploration. Where a single species of tree is common and widespread it has the potential advantage over traditional media, such as tills and soils, in that it has a matrix that is compositionally consistent over large areas, and thus, provided samples of similar appearance and consistency are collected, it is less prone to the hard-to-interpret variations caused by matrix variability encountered in other media. Once sap has congealed on the tree bark it is chemically inert, easy to find and quick to sample, including in recent clear cut areas where it can be found on fallen logs and tree stumps.

This project tests the viability of using white spruce (*Picea glauca*) sap as a sample medium for regional exploration. In the François Lake area of central BC, the chosen field area for this study, white spruce is the dominant tree species. The study area includes the Endako molybdenum mine and Nithi Mountain molybdenum prospect that represent suitable test sites. Furthermore regional-scale pine bark biogeochemistry surveys carried out by the Geological Survey of Canada (GSC) in the late 1990s provide a robust historical dataset against which the results of the tree sap sampling can be compared.

Additional components to the study include a comparison of element concentrations in sap from white spruce and lodgepole pine (*Pinus contorta*) and the organic-rich Ah horizon. The latter comprises a combination of decaying plant material, bacteria, exuded fluids, and particulates, such as wax coatings to leaves that have been shed from tissue surfaces. It is also believed to be a sink for upward-moving ions from underlying bedrock. As such it is a rich milieu of chemically-reducing organic material that contains metals from these various sources.

OBJECTIVES

This project set out to address the following questions:

1. Does sap provide information of value to mineral exploration in glaciated terrains?
2. If so how does the usefulness of this information compare to other available sample media?
3. Can saps be used as a reliable sample medium in contaminated near-mine environments?
4. What are the recommended sampling strategies for the collection of saps?
5. What is the optimal sample preparation and analytical procedure to be employed for obtaining precise data?
6. What levels of detection are required to see the geochemical signatures of saps?
7. How does the geochemical signature of sap compare to signatures from those of organic-rich soils (Ah horizon) and of bark tissues (data obtained from previous surveys), and is the signature from saps more definitive than other media for delineating known mineralization?
8. Do saps from pines provide similar information, and can the data from different species be integrated or do they need to be levelled for comparison?

BENEFITS TO THE MINING INDUSTRY

This study is designed to provide the mineral-exploration community with an understanding of the potential advantages of sampling saps from common conifer trees in the exploration for mineral deposits in regions with glacial sediment cover. It provides comparisons of metal concentrations in saps, Ah-soil horizon and pine bark tissues and assesses the relative capabilities of each medium for preserving the secondary geochemical dispersion patterns related to a buried mineral deposit. The study assesses the value of this alternative sampling medium for local- and regional-scale geochemical sampling programs in areas where conventional soil-sampling methods might be found ineffective and/or where contamination from mining activities might present a problem to the use of other geochemical exploration sampling media.

Previous Studies

Kyuregyan and Burnutyan (1972) demonstrated that plant saps could be used in the exploration for Au, and the sap Au content was significantly higher than that of other extracts of the plant material or extracts from the underlying soil. Saps from birch species are the most studied, both because of the ubiquity of birch in the boreal forests (especially Siberia and Finland) and of their strong sap flow in the spring.

Krendelev and Pogrebnyak (1979) conducted a sampling program in an area of permafrost over an intensively fractured and hydrothermally-altered Au-mineralized stockwork in Transbaikal, where Au mineralization is associated with pyrite and is situated beneath 0.5–4 m of unconsolidated sediments. The Au content from analysis of 73 samples was reported as 0.011–0.33 ppb, demonstrating a 30-fold range in concentration. In the same study, over a zone of Zn-rich ore, concentrations in fresh sap reached 17.2 ppm Zn. The authors observed that in the vascular system of the birch species studied (*Betula platyphylla*) there was no biological barrier against the absorption of Zn and concluded that the best anomaly to background contrast was obtained by calculating the Zn/(K+Ca+Mg) ratio.

Harju and Huldén (1990) conducted an exhaustive survey in southern Finland where they collected sap samples from many species of birch (mostly *Betula verrucosa*) over a 10-year period. Sap samples collected along transects over a zone of base-metal–rich skarn mineralization revealed clear anomalies for Ag, Cd and Zn above the mineralization (Fig. 1). Furthermore, they stated that Pb values were highest at sites closest to the mineralization, whereas the Cu concentrations produced a less distinct Cu anomaly. More details of the use of saps in exploration are summarized in Dunn (2007)

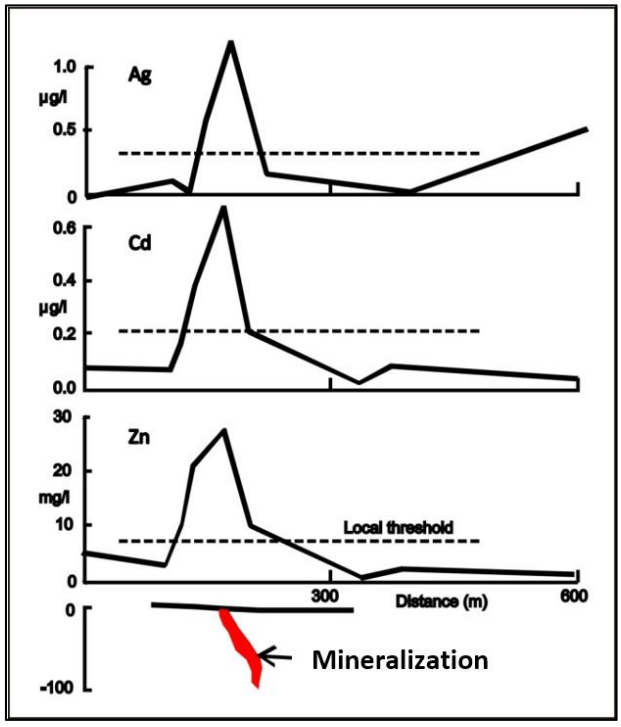

Figure 1. A transect across a skarn-type polymetallic sulphide deposit in Finland. Concentrations in birch sap (Betula verrucosa) of Ag, Cd and Zn (after Harju and Huldén, 1990)

Studies conducted under the auspices of Geoscience BC (Heberlein *et al*., 2013) have indicated that once a plant has assimilated those elements that it requires for its growth and health, excess amounts of elements may be exuded via saps and transpired fluids. Furthermore, 'toxic' elements that are commonly of use as pathfinder elements in mineral exploration (e.g. Hg, As, Sb, Tl and W) tend to move through a

plant with a relatively large portion of those taken up by the root system being transpired with plant exudates (saps, other fluids and particulates).

Study Area and Pre-mining Biogeochemical Studies

The area chosen for this study lies in the northern Nechako plateau region of Central BC (parts of NTS map sheets 093F14, 093F15, 093K02 and 093K03). It overlaps the northern boundary of the Geoscience BC TREK project area as shown in Figure 2. It is centred on the Endako Mine and Nithi Mountain prospect and contains a number of other mineral occurrences containing Mo and Zn, and a few Cu and Au occurrences (Fig. 3).

The town of Fraser Lake, located in the northeast of the study area, was used as the main logistical centre for the sampling program. Access for sampling was from Highway 16, the main route joining Prince Rupert and Prince George, and a network of other roads, including forest service, logging and the main access road to the Endako Mine. Limited access to the west of the mine and in François Lake Provincial Park on the south shore of François Lake, precluded sampling of those areas.

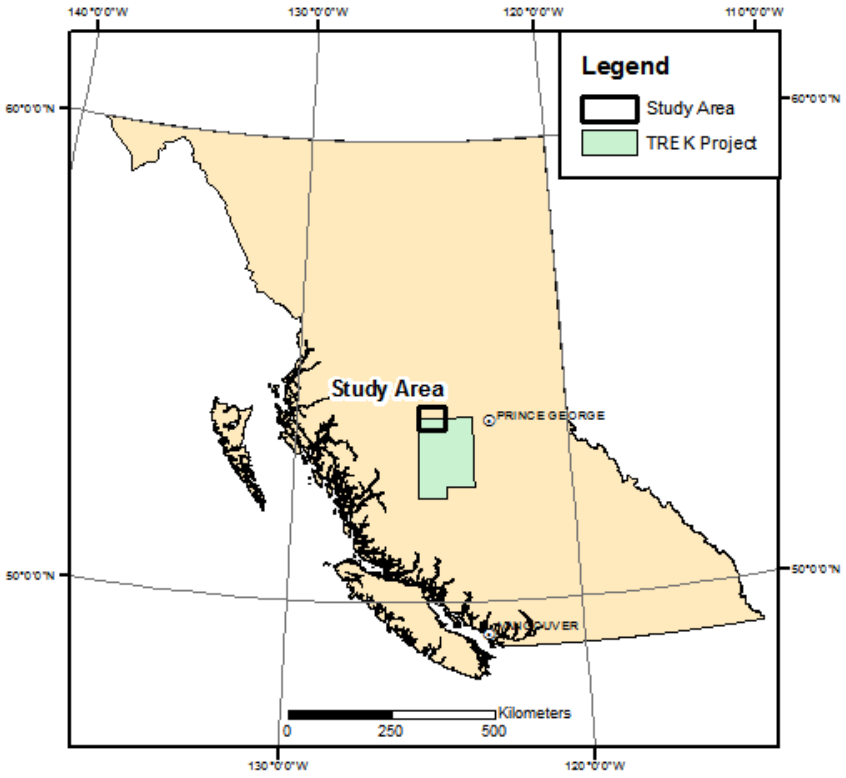

Figure 2. Location Map showing the TREK Project and the area described in this report

With regard to the selection of the Endako Mo mine as the focus for this study, it is relevant to note that biogeochemical studies were first carried out in this area in the early 1950s more than a decade before any drilling was conducted (Warren *et al*., 1953). These investigations identified a strong Mo signature, prior to disturbance by exploration activities, with concentrations in dry subalpine fir needles and stems

of 65 ppm and 43 ppm, respectively. Compared to areas in BC with no known Mo mineralization, these concentrations represented values about 500 times background levels. Later surveys conducted soon after early mining activities commenced disclosed some extraordinarily high concentrations of Mo in unidentified species of willow (*Salix* sp.) and fireweed (*Epilobium angustifolium*) with a maximum concentration in the latter of 17,000 ppm Mo in ash (Warren and Delavault, 1965). This represents approximately 300 to 500 ppm Mo dry weight. Samples of fireweed collected from outside the mine perimeter more than 30 years later after extensive mining activity found 2950 ppm Mo in ash (approximately 60 to 100 ppm dry weight), indicating a sustained anomalism but with concentrations much lower than had previously been recorded (Dunn, 1998, 2007). Additional biogeochemical anomalism was found in samples of pollen collected in 1980 and 1981 with 48 ppm Mo and 41 ppm Mo (dry weight), respectively (Warren and Horsky, 1982). These valuable historic data demonstrate that Mo enrichment in the vegetation was present long before mining activities commenced, and those mining activities have not enhanced the Mo environmental signature. As a result, it is assumed that the sap signature described in this report may well represent a natural level of Mo in this area.

SURFICIAL ENVIRONMENT

The study area lies in the central part of the Nechako Plateau at the northern end of the Interior Plateau of central BC (Holland, 1976). It is an area of moderate relief characterized by rolling hills and relatively steep sided valleys. Elevations range from 676 m at Fraser Lake to 1370 m due west of the Endako Mine (Fig. 3). The terrain is slightly more rugged in the southern part of the area, south of François Lake, than to the north of the lake where the Endako River valley defines a broad lowland area dotted by numerous small lakes and wetlands (Plouffe, 2007).

Surficial Geology

The Nechako Plateau was ice-covered during the last glaciation and consequently much of the study area is blanketed by different types of glacially-derived sediment (Fig. 3). The Endako River valley in the north is underlain by a blanket of glacial till that has a distinctive fluted and grooved surface caused by swarms of east-west drumlinoid landforms that strongly influence local drainage patterns. Hillsides are also till-covered but to a much lesser extent. Much of the area to the south of François Lake has a till veneer that thickens locally to a till blanket close to valley floors.

The main valleys are orientated east-west, reflecting the predominant ice-flow direction from the west (Ferbey *et al.,* 2013). Surficial deposits at the east end of François Lake and around Fraser Lake include glaciolacustrine sands and gravels as well as deeper water silt and clay deposits that were laid down when the lakes covered much larger areas than they do today.

Outcrops are few and far between and are generally restricted to the highest elevations and steepest slopes. Colluvial deposits are present on the southern slopes of Nithi Mountain and along the upper reaches of the Stellako River joining Fraser and François Lakes.

Soil Profiles

Soils are poorly developed, and most profiles encountered during the two sampling campaigns belong to the Regosolic order. They are present on all substrates, including the tills and glaciolacustrine deposits mentioned above. Surface leaf litter (LFH) lies on top of a variably developed Ah horizon. Depending on the degree of site drainage, the Ah horizon can vary from non-existent at very dry sites to several centimeters thick where drainage is poor. Rare brunisols are encountered at some localities particularly on steep hill sides and in poorly drained upland areas. Podzol profiles are very rare, occurring only in upland areas west of the Endako mine.

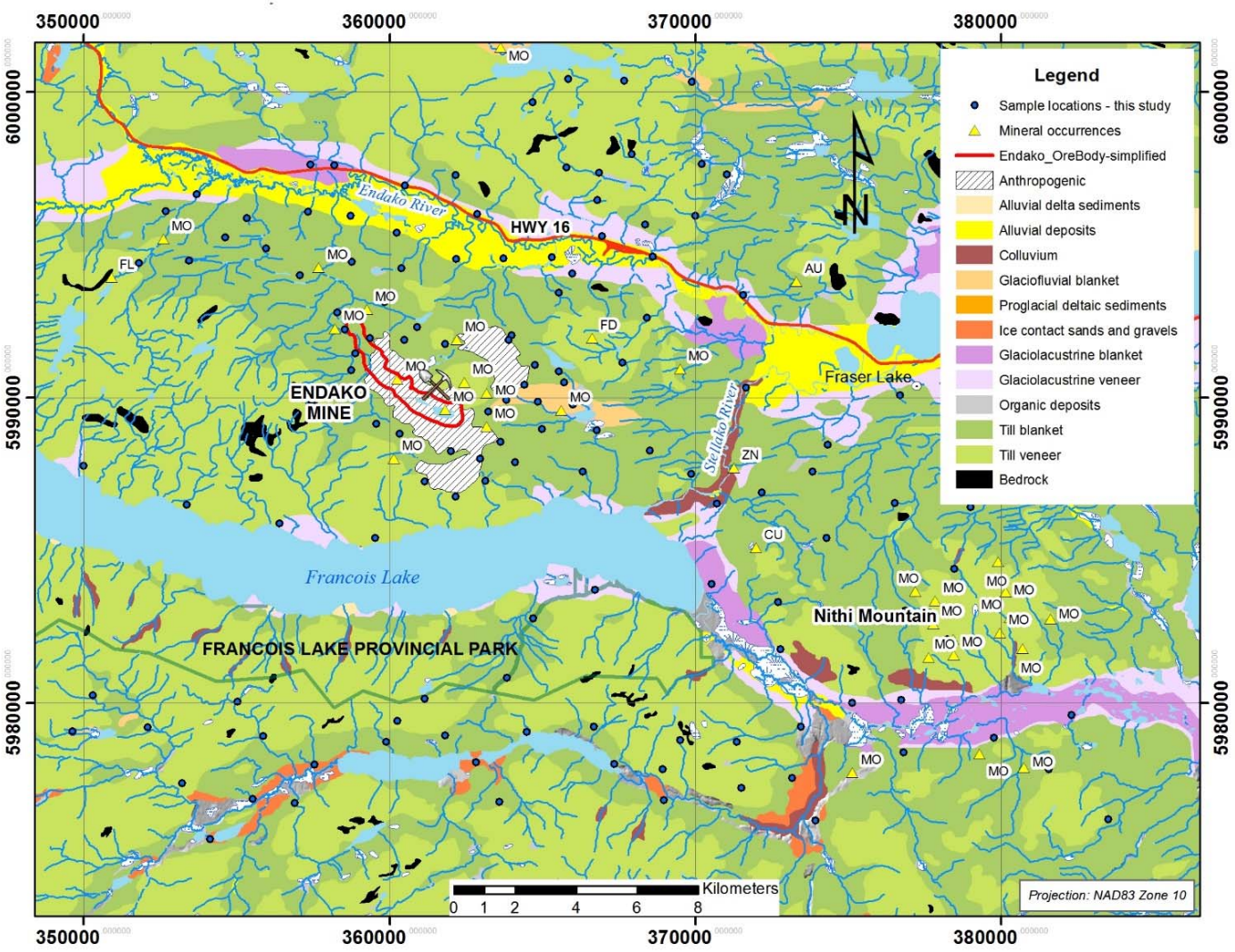

Figure 3 Simplified surficial geology of the study area (after Plouffe, 2007). Mineral occurrence abbreviations: FL – Fluorite, MO – Molybdenite, CU – Copper minerals, AU – Gold, ZN – Zinc minerals

Vegetation and Climate.

The survey area falls into the Sub-Boreal Spruce biogeoclimatic zone (BC Ministry of Forests, 2014; (ftp://ftp.for.gov.bc.ca/HRE/external/!publish/becmaps/PaperMaps/BGCzones.8x11.pdf). The continental climate has extremes of temperature reaching above 30^{o} C in the summer, with prolonged periods below -10^{o}C and sometimes dipping below -40^{o} C in the winter. Much of the region is under a thick snow cover from November to March.

This extensive biogeoclimatic zone occurs in the central interior of the Province, primarily on gently rolling plateaux, and extends from the Rockies to the Coast Mountains. White spruce (*Picea glauca*) is the dominant coniferous tree species and is interspersed with extensive stands of lodgepole pine (*Pinus contorta*) in the drier areas, and subalpine fir (*Abies lasiocarpa*) at higher elevations. Because of the devastation caused by mountain pine beetle in recent years, live pines are uncommon. Subalpine fir is sparse throughout the survey area. White spruce locally hybridizes with Engelmann spruce (*Picea engelmannii*), but distinctions are difficult to identify and previous unpublished studies (data obtained by the second author) have found no obvious differences in the chemistry of the white spruce and the hybrids. Given that the Engelmann spruce forests are more prevalent a considerable distance to the southeast of the survey area, for the purposes of this report all spruce are referred to as white spruce, although the more generic term 'interior spruce' could be used.

Deciduous species are present as isolated occurrences or small stands and are common along roadsides and drainages. The most dominant species are trembling aspen (*Populus tremuloides*), black cottonwood (*Populus balsamifera*) and paper birch (*Betula papyrifera*). The understory has a wide range of shrubs, especially Sitka alder (*Alnus sitchensis*). The forest floor has a cover of mosses consisting mostly of feather-moss (*Pleurozium schreberi*) and step moss (*Hylocomium splendens*).

This report focuses on white spruce, with some comparative data from neighbouring lodgepole pines.

GEOLOGY

Regional Setting

Villeneuve *et al*. (2001) provided a comprehensive summary of the episodic plutonism of the Endako Batholith and the age of the molybdenite mineralization. The following is extracted largely from their study.

The Endako batholith has been divided into three Mesozoic suites on the basis of geological mapping supplemented by geophysical and geochemical studies conducted mostly in the late 1990's. The survey area is underlain largely by this composite batholith which Villeneuve *et al*. (2001) divided into:

1. Stern Creek plutonic suite (~220 Ma – Late Triassic); foliated hornblende +/- biotite diorites and gabbros. These intrude upper Paleozoic amphibolite, schist, and ultramafic rocks of the Taltapin metamorphic complex;
2. Stag Lake plutonic suite (~181-170 Ma – Middle Jurassic) with four intrusive intermediate to mafic phases. This heterogeneous plutonic suite is marginal to much of the Endako batholith and has compositions ranging from gabbro to quartz-monzonite.
3. François Lake Plutonic suite (~157-145Ma – Late Jurassic). This suite forms the bulk of the exposed batholith and is the host rock to the Endako molybdenite deposit. Compositions are more felsic than the older phases ranging in composition from granite, syenite, and monzonite to tonalite. A major phase in this suite, located at Nithi Mountain, was intruded ~155 Ma. This is the Glenannan sub-suite containing significant occurrences of porphyry-style molybdenite mineralization.

Small post-Jurassic granodiorite to quartz monzonite stocks are scattered through the region. They are represented by the late Cretaceous Holy Cross and Cabin Lake plutons on the south side of François Lake and the Eocene Sam Ross Creek Pluton that occurs as two separate intrusions west of the Endako mine.

Volcanic and sedimentary rocks of various ages are present in the southern, northwestern and northeastern parts of the map area. Oldest volcanic rocks are Early to Middle Jurassic Hazelton Group, trending east-west and outcropping south of François Lake. Late Cretaceous-age Kasalka Group andesitic volcanics overlie the Hazelton Group and cover much of the area along the south shore of François Lake, and west of the Endako Mine on the north side of the lake. They consist of a predominantly subaerial sequence of grey-green to purple andesite flows and associated pyroclastic rocks. Cenozoic volcanic rocks are also widespread throughout the map area. They are represented by the Eocene to Oligocene Ootsa Lake Formation in the southwest and the Endako Formation in the northeast of the map area. Ootsa Lake Formation consists of predominantly felsic volcanic rocks characterized by flow banded and spherulitic rhyolites with minor fragmental units. Endako Formation rocks consist of vesicular to amygdaloidal basaltic andesite flows. The Cenozoic rocks are mostly preserved in down-dropped fault blocks.

Mineralization

Although the first claims were staked in 1927 and the area was examined by many prospectors, geologists and some mining companies over the ensuing years, it was not until 1962 that the first diamond drilling programs were carried out. Subsequently, many studies of the molybdenite mineralization hosted by the Endako batholith have been conducted.

Mineralization is categorized as low-F-type porphyry Mo, for which a typical geochemical signature is Mo, Cu and W. At least ten mineralized phases, based on distinct textural and compositional changes, have been recognized in the composite batholith. The orebody consists of an elongate stockwork of quartz-molybdenite veins developed within the Endako quartz monzonite phase and three types of felsic pre-mineralization dikes (BC Ministry of Energy MINFILE No. 093K 006). The primary ore mineral is molybdenite (MoS_2), which occurs with minor chalcopyrite, scheelite, and galena. Gangue minerals

include quartz, pyrite, K-feldspar, biotite, sericite, clays, calcite, and anhydrite. Villeneuve *et al.* (2001) note that although the primary molybdenite mineralization at Endako is tied to the latest stage of Jurassic plutonism, the actual source of the mineralizing fluids remains enigmatic. Textural evidence supports the existence of potentially three ages of mineralization that have been dated using the Os-Re method (Selby and Creaser, 2001) at 154 Ma, 148-146 Ma and ~145 Ma respectively. The close relationship between these ages and the ages of granitic phases of the Endako batholith (e.g. Nithi, Endako and Casey phases) suggest a genetic relationship between the mineralization and these apparently coeval plutons.

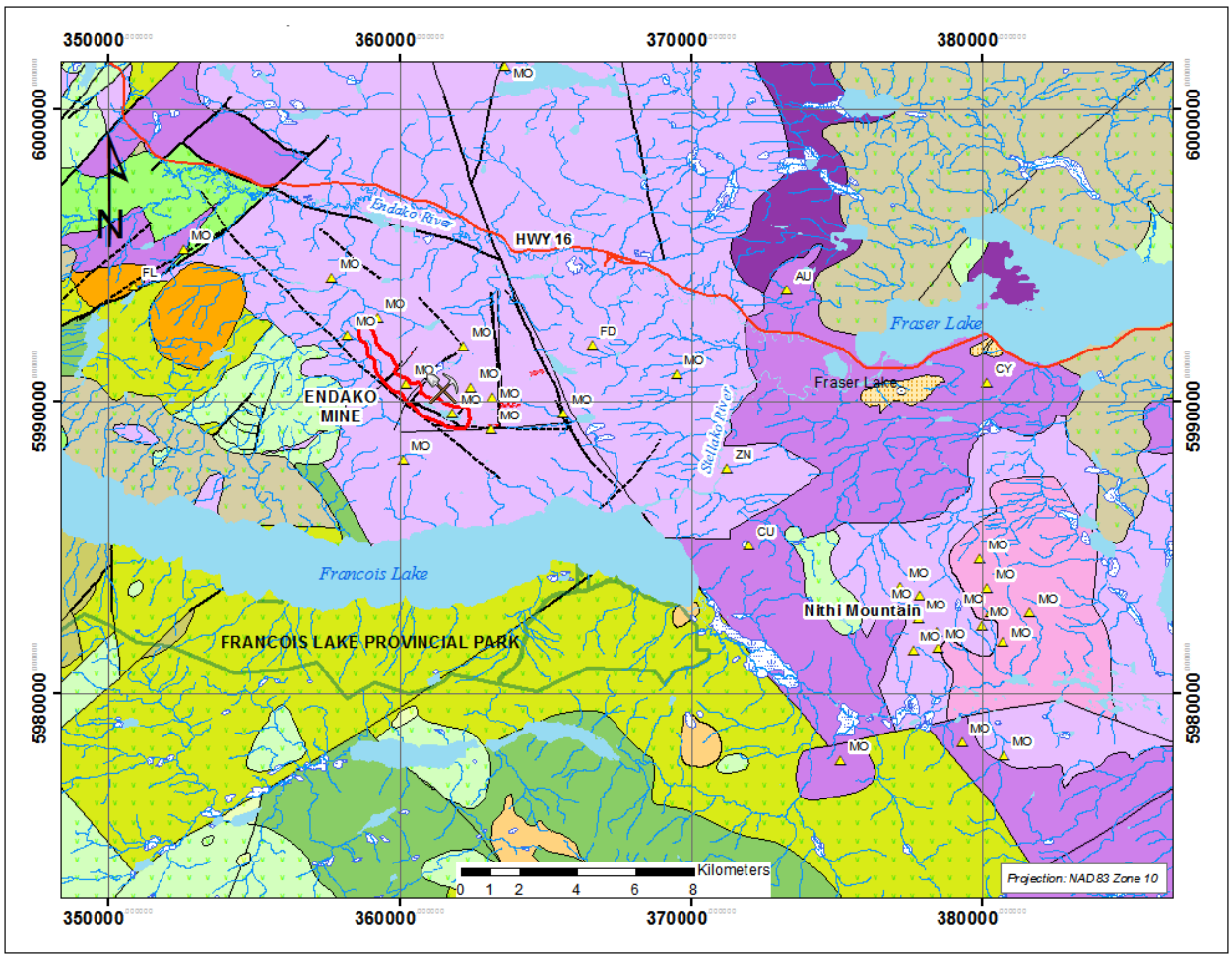

Legend

Volcanic and sedimentary rocks

- Eocene to Oligocene, Nechako Plateau Group - Ootsa Lake Formation
- Eocene, Nechako Plateau Group - Endako Formation
- Late Cretaceous, Kasalka Group
- Lower Cretaceous, Skeena Group
- Middle to Late Jurassic, Bowser Lake Group
- Early to Middle Jurassic, Hazelton Group

Intrusive rocks

- Eocene, Sam Ross Creek Pluton
- Early Cretaceous, Endako Batholith - Fraser Lake Suite - Fraser Phase
- Late Jurassic, Endako Batholith - Francois Lake Suite - Glenannan Subsuite - Nithi Phase
- Middle Jurassic, Endako Batholith - Stag Lake Plutonic Suite - McKnab Phase
- Middle to Late Jurassic, Endako Batholith - Francois Lake Suite
- Late Triassic, Stern Creek Plutonic Suite - Stern Creek Phase

- Sample locations - this study
- Mineral occurrences
- Endako orebody

Figure 4 Geology of the study area (simplified from BC OF2013-4)

FIELD PROGRAM

The field program was designed as a regional geochemical survey over Endako and northern parts of the TREK project area (Fig. 1). Sap samples (~2g, mostly white spruce but with a few lodgepole pine for comparison) and Ah horizon soil were collected at an average sample density of one sample per 4 km^2 except in the immediate vicinity of the Endako mine where samples were more closely spaced. Sample sites corresponded with part of a GSC lodgepole pine bark biogeochemistry survey that was carried out over the area in 1997 and 1998 (Dunn and Hastings, 1998a, b, c, d and 1999a, b, c, d). This historical survey provides a comparative data set from another sample medium to compare with the results of the sap analyses. Activation Laboratories (Actlabs), Ancaster, Ontario, developed the methodology for the sap analysis, and Acme Analytical Laboratories in Vancouver (Acme) analyzed the Ah horizon samples.

Sampling

Sampling was initially undertaken during a five day period in September, 2013. Ah horizon samples and saps were collected from 116 and 108 (98 spruce and 10 pine) locations respectively, corresponding to as many of the 1997-98 lodgepole pine bark sample sites that could be reached by roads and trails. Not all of the planned locations could be sampled, because many of the forestry roads that were accessible in the late 1990s had either been decommissioned or had overgrown to such an extent that safe access was not possible. In such cases alternative sample locations were selected as close to the originals as possible.

Globules of sap were found to be present on most of the spruce trees in the survey area. They tend to accumulate as clean discrete globules of amber to yellow resinous material that can quite easily be picked off the surface with the point of a penknife. Other tools, such as a paint scraper, are unsuitable because they tended to include too many bark particles in the sample. It proved useful to have a container such as a dustpan into which the globules could be collected (see frontispiece). The small bark particles were winnowed away by gently blowing into the dustpan. The cleanest material was then hand-picked and placed into vials for transportation to the laboratory. This procedure resulted in samples with few exotic fragments and the 'clean' congealed sap could be sent for analysis. Each sample took only a few minutes to collect ~2 g into a glass vial.

At some locations where white spruce trees were not present, lodgepole pine sap was collected instead. Both pine and spruce saps were collected at a small number of sites for comparative purposes in order to assess whether the two species have similar sap compositions, or perhaps linear relationships that would allow for correction of pine to a spruce equivalent value where spruce is unavailable

For logistical reasons no samples were collected from the Endako mine site during the initial sampling campaign, and thus a second sampling expedition was necessary with the help of Michael Pond (Endako Chief Geologist) from Thompson Creek Metals Company Inc. (Thompson Creek) to obtain coverage from inside the mine fence. This was completed between May 9th and 11th, 2014, and involved sample collections from an additional 22 stations.

Figure 5 illustrates the sampling coverage from the two campaigns and the locations of the 1998 pine bark samples. A summary of the numbers and types of samples collected in both campaigns is shown in Table 1.

Table 1. Summary of Field Samples

	Spruce Sap	Pine Sap	Sap Field Dups	Ah Soils	Ah Field Dups
First campaign	98	10	9	116	11
Second campaign	22	2	3	21	2

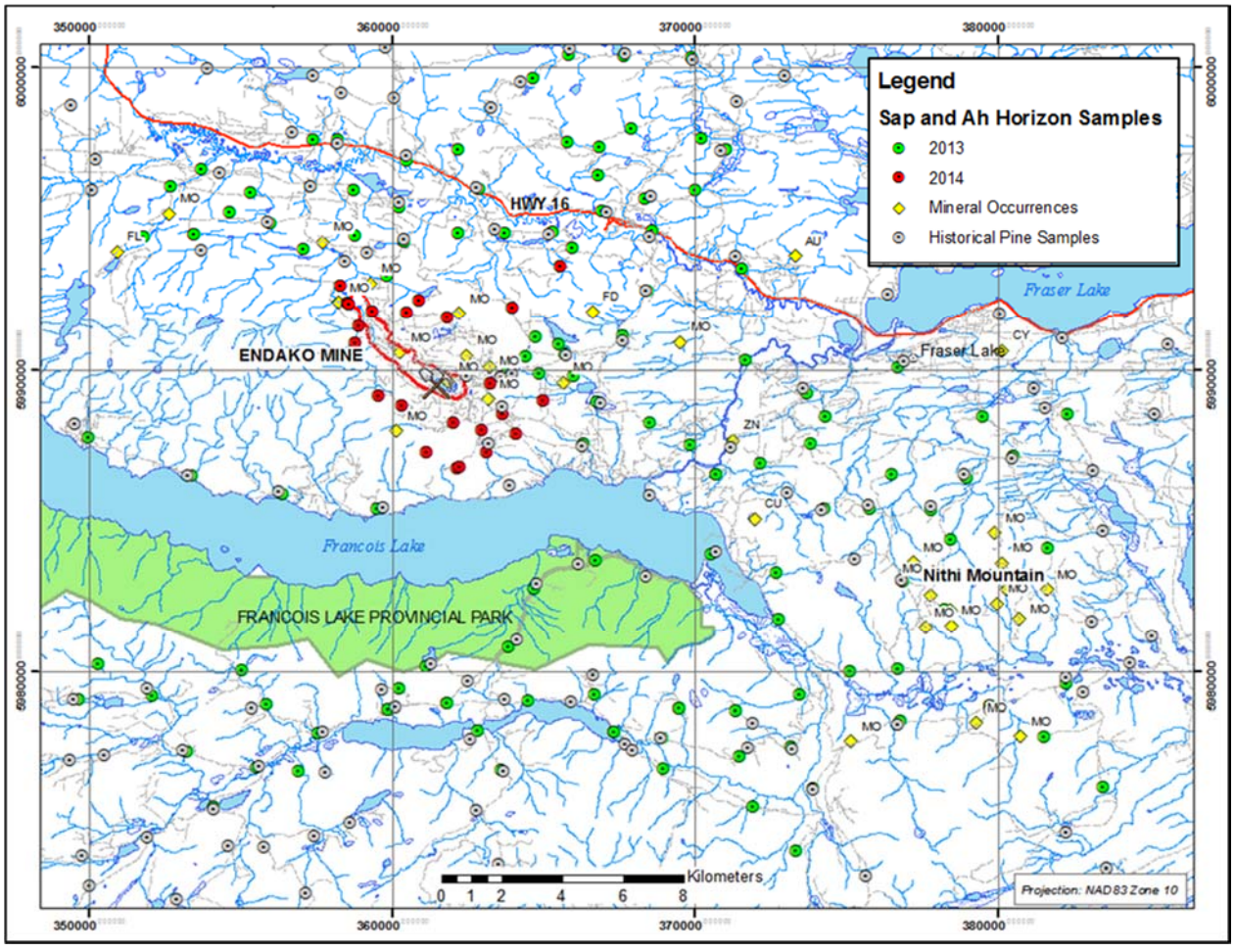

Figure 5. Sample location map showing 1998 pine bark samples (grey), 2013 sap and Ah samples (green) and 2014 samples (red).

ANALYTICAL METHODS

Soil pH Measurements

Samples for soil pH measurements were collected at each sample site (Fig. 5). Approximately 50 g of material was collected from the top centimetre of the leached Ae horizon, or from the top of the B horizon where the Ae horizon was either absent or poorly developed (e.g. in brunisol profiles). Care was taken to avoid organic-rich material from the overlying Ah horizon as organic acids can interfere with or mask the sought-after bedrock responses. Samples were placed in heavy-duty double-seal Ziploc® plastic bags.

Soil pH measurements were made on 1:1 slurries of soil and distilled water. Approximately 20 mL of soil was placed in a graduated plastic beaker and the volume was brought up to 40 mL with distilled water. The mixture was thoroughly stirred. Readings were taken on the slurry after 20 seconds using an Oakton Industries pH Testr 30 portable pH meter. The meter was soaked in tap water overnight prior to taking the readings. A three point calibration was made before the pH readings with pH 4.01, 7.0 and 10.1 NIST pH buffer solutions; pH values were converted to H^+ ion activities for plotting.

Ah Horizon Samples

Ah horizon samples were sent to Acme Analytical Laboratories in Vancouver, where they were air dried and screened to -80 mesh. A 0.5 g aliquot of the -80 mesh fraction was analyzed by ICP-OES and ICP-MS after digestion by a modified aqua regia (formerly Acme's Group 1F04 method, now referred to as AQ250-EXT).

Sap

There is no 'off the shelf' commercial method for the digestion of tree saps. For a recent study at Woodjam (Heberlein *et al*., 2013), the saps were microwave-digested in nitric acid at Queen's University (QFIR). While effective at bringing the entire sample into solution, this method is also likely to dissolve dust contaminants, which could interfere with the sought-after geochemical signal. Left-over sap samples from the Woodjam project were used for experimentation and optimization of the digestion method.

Visual and microscopic characteristics of sap.

The Woodjam materials used for the early digestion tests were found to be atypical of the sample collection as a whole; they were quite milky in appearance and did not readily dissolve in a variety of organic solvents and acids[1] (Fig. 6). The large majority of samples collected for the Endako survey were

[1] Dissolution tests were performed using acetone, methyl alcohol, ethyl alcohol and different ratios of nitric acid, perchloric and hydrochloric acids.

amber in colour and transparent, having a similar appearance to the frontispiece of this report. A few samples were milky in appearance and were noted on the field sheets (Table A1, Appendix 1)

Under the scanning electron microscope some milky samples were found to contain solid residue, such as the calcite grains and calcium oxalate (CaC_2O_4) crystals shown in Figures 6 and 7.

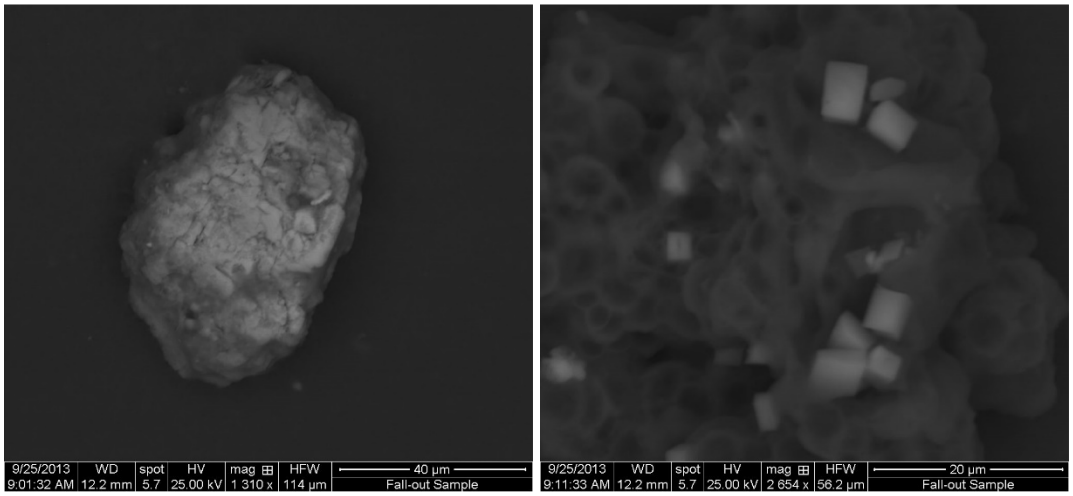

El	AN	Line	unn. C [mass %]	norm. C [mass %]	Atom. C [At.%]
C	6	K-series	11.21	14.44	24.74
O	8	K-series	31.09	40.06	51.53
Mg	12	K-series	0.69	0.90	0.76
Al	13	K-series	0.25	0.32	0.24
Si	14	K-series	0.47	0.60	0.44
P	15	K-series	0.00	0.00	0.00
S	16	K-series	0.00	0.00	0.00
Cl	17	K-series	0.00	0.00	0.00
K	19	K-series	0.28	0.36	0.19
Ca	20	K-series	32.79	42.25	21.70
Fe	26	K-series	0.84	1.08	0.40
		Total::	77.6 %		

Figure 6. An SEM backscatter image of a calcite grain (top left, with analysis underneath) and Ca oxalate crystals (top right) encapsulated within congealed 'milky' sap

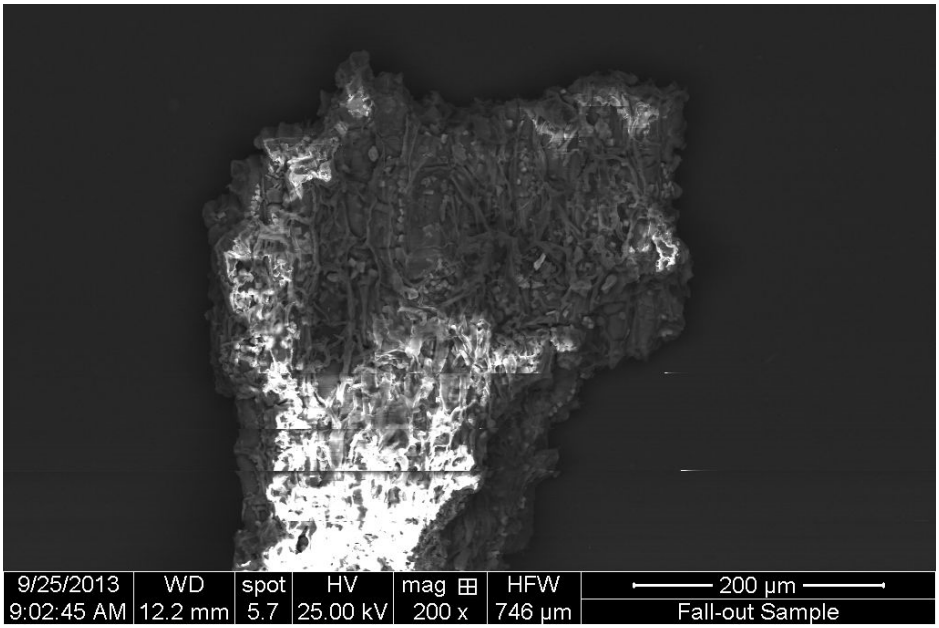

El	AN	Line	unn. C [mass %]	norm. C [mass %]	Atom. C [At.%]
C	6	K-series	62.47	62.47	72.33
O	8	K-series	28.28	28.28	24.58
Mg	12	K-series	0.57	0.57	0.33
K	19	K-series	0.89	0.89	0.32
Ca	20	K-series	6.72	6.72	2.33
		Total::	100.0 %		

Figure 7. A back scattered electron microscope image showing complex structures in congealed sap. The white material is probably with Ca oxalate (CaC_2O_4).

Because of these insoluble components, particular care was taken to select fragments for analysis which were clear and devoid of particulate matter. This involved some careful collection in the field followed by further refinement in the laboratory by centrifuging after dissolution to ensure that only the pure sap was submitted for analysis.

Figure 8 shows an impure sap sample which, on the right, has been filtered through a 0.45 µm filter. The filtered residue is shown on the left. It is the filtrate on the right that was subjected to the final analysis.

Figure 8. Filtered residue (left) and purified sap sample after filtering (right)

After extensive experimentation including the use of various digestion procedures and the microscopic examination of residues, Actlabs has developed a methodology to selectively dissolve the saps while minimizing dissolution of contaminant particles. Optimization of the sap digestion method was undertaken on left-over samples from the Woodjam project as well as on a bulk sap sample collected from the Endako area. Once the best technique had been identified, samples from both sampling campaigns were run together as a single batch to eliminate the possibility of batch effects.

Analysis

The analytical procedure was arrived at following experiments with various digestions and analytical instruments. Both HR ICP-MS and two makes of quadrupole ICP-MS were tested to find the optimal instrument: it was observed that sap samples behaved differently with the different makes of instrument, generating different detection levels and analytical results. The sample dissolution procedure used for the final analysis was as follows:

- Samples were spread on a piece of lint-free paper towel: the pure sap portions were hand-picked (to exclude other material such as bark fragments) and placed in pretested acid-washed Teflon test tubes for weighing.
- A 0.25 g aliquot of sample was accurately weighed.
- The sap was then completely dissolved in methanol and the resulting solution filtered through a 0.45 µm membrane to remove potential particulate contaminants, and collected into a second pre-weighed clean and dried Teflon tube.

- The Teflon tubes were placed in two racks which were transferred to a single heat block to evaporate the methanol to dryness at 120^{o} C.
- Once the content was dried, the tube was weighed again. The difference in weights was the sap mass used for concentration calculation. The extraneous material coarser than 0.45 µm was discarded.
- All samples were then digested in a HNO_3/$HClO_4$ acid mixture at 190^{o} C and then slowly ramped up to 260^{o}C and held at that temperature for 1.5 hrs. A plastic watch glass was placed on each tube to create reflux. Additional HNO_3/$HClO_4$ was added if the digestion was incomplete.
- Once the digestion was completed, the solution was evaporated to near dryness.
- The contents were re-dissolved in aqua regia and further diluted prior to analysis.
- Final dilution was about 60-fold to try to maintain the best detection limits and still not have excessive suppression due to matrix effects. Suppression was monitored with Rh and Ir internal standards.
- Samples were injected into the ICP-MS by flow injection using an ESI auto-sampler to minimize effects on suppression.
- For the final analysis an Agilent 7700 ICP-MS was used because it was found that the solutions could be run with the least dilution on this particular instrument due to its ability to handle high total dissolved solids content without appreciable suppression. This instrument also minimized any normal ICP-MS interferences from oxides or chlorides using the dual gas/no gas modes.

QUALITY CONTROL MEASURES

Quality control measures used for the field sampling campaigns included the collection of field duplicate samples and, for the Ah samples, the insertion of a certified reference material (CRM). There are no suitable CRMs for tree saps, and so Actlabs used a vegetation control sample, NIST 1575a (pine needles), as an internal control. Digestion of this material was found to be partial (about 60% recovery for most of the 20 elements for which certified values are available), and so the analyses gave only a very limited assessment of analytical precision and accuracy. Assessment of precision was only possible from consideration of data from the field duplicate samples.

Field duplicates were collected at a frequency of approximately one in every 10 field sample sites. Duplicate sampling involved the collection of a second sap and Ah horizon samples from within a 5 m radius of each original. CANMET's LKSD-4 reference material (an organic-rich lake sediment with similar characteristics to Ah horizon soil) was used to monitor accuracy, precision, drift and bias in the Ah horizon results. Brown sugar crystals were attempted to be used as a drift monitor for the sap samples, but unfortunately this material was found to be insoluble in the final digestion. Therefore bias in the sap results could not be monitored.

DATA QUALITY

An unacceptably high total measurement error can undermine the ability of a geochemical technique to detect mineralization by obscuring meaningful geochemical patterns (Abzalov, 2008; Stanley and Smee,

2007). Sources of measurement error include: a) sampling error; b) preparation and subsampling error; and c) analytical error. Errors attributed to each stage of the sampling and analytical process are additive with sampling error, which is a measure of the representivity of a sample of the material being sampled, accounting for by far the largest proportion of the total in this study, usually more than 80%.

Total measurement error is expressed as the average coefficient of variation, or CVav which is calculated using the following formula (Abzalov, 2008):

$$CV_{AVR}(\%) = 100 \times \sqrt{\frac{2}{N}\sum_{i=1}^{N}\left(\frac{(a_i - b_i)^2}{(a_i + b_i)^2}\right)}$$

Where a and b represent the original and duplicate analyses and N the number of duplicate pairs. Values can range from 0%, when duplicate pairs have identical concentrations, to an upper value of 141.21% (i.e. the square root of 2) when duplicate results exhibit maximum differences. For the purpose of this study, values of below 20% indicate good data quality; between 20 and 30% acceptable quality; between 30 and 50% marginal quality; over 50%, poor quality. Elements falling in the poor category must be used with caution as their patterns are likely to be influenced by noise caused by poor reproducibility.

Ah Horizon

Table 2 shows the total measurement error values of the Ah horizon field duplicate analytical results. Values are colour coded as a function of overall data quality with poor quality results highlighted in red, marginal quality in gold, acceptable quality in blue and good quality in black. Seven elements, As, Au, Mn, Re, Se, Te and Tl, display total measurement errors at or above 50%; however, of these elements only As and Au have values significantly above this level. Gold has the highest total measurement error of 70.50%. This almost certainly reflects a nugget effect caused by the random distribution and size of gold particles in the soil. A value of 64.14% for As is more difficult to explain. This element does not occur in particulate form in the secondary environment and thus a nugget effect is considered unlikely. A more likely explanation is the proximity of the values to the method detection limit (0.1 ppm) where random error is greatest. The same explanation applies to Re, Se and Te where the majority of values fall close to their respective detection limits (see Appendix 1).

Elements with marginal data quality (shaded gold) include Ag, Bi, Cd, Co, Cu, Li, Mo, Nb, Rb, S, Sc, Th, U, V, Y, Zn and Zr. Once again, the higher total measurement errors are attributed to their concentrations being close to their analytical detection limits. Interpretation of the results for these elements should be done bearing in mind that patterns are expected to be quite erratic because of the relatively high measurement errors. The remaining elements have good to acceptable data quality and are suitable for plotting and interpretation with confidence as to their distribution patterns.

Table 4 summarizes the results for the CANMET LKSD-4 reference material that was included as a control for the Ah horizon samples. Not all of the analytes have certified values for this reference; those that do are included in the 'Accepted' value column. The table shows the mean of the LKSD-4 determinations

and, where applicable, the relative bias from the accepted value. It also includes the percent relative standard deviation, or RSD%, which is a measure of the precision of the analyses. The accepted values are based on a dilute HNO_3-HCl partial extraction and ICP-MS finish (http://www.nrcan.gc.ca/mms/canmet-mtb/mmsl-lmsm/ccrmp/certificates/lksd-1.htm). Missing values indicate elements for which no data are published.

Results show that the averages are within ±20% of the accepted value for most certified elements. Exceptions include Ag (+21.5%), Mo (-25.3%) and Sb (-52.16%). The negative bias for the majority of elements suggests that the AQ250 extraction is weaker than the two acid digestion used by CANMET.

Precision, shown by the percent average Coefficient of Variation (CVav%), is below 10% for most elements indicating a high degree of reproducibility for the reference material. Poorer precision occurs for Au (38%), Be (23%), Hf (14%), In (27%), Mo (11%), Na (14%), Re (47%), Te (48%) and Th (12%). However, since for this study the patterns of relative element concentrations for a given element (i.e. precision) are of greater significance than the absolute values (i.e. accuracy), these discrepancies are of low significance for interpretation of the results. Higher CV values for Au are attributed to a nugget effect caused by its occurrence as randomly distributed particles. For the other elements, the higher RSD% values are the result of their concentrations being at or close to their respective detection limits where analytical precision is poor (Table 3). Of importance to this study is that many of the anomalous values are concentrations well above detection limits, such that their reproducibility is much better than at the low, poorly repeatable, levels that the statistics indicate.

Table 2. Total measurement errors for Ah Horizon soil results (N=12); black = <20%; blue = 21-30%; gold 31-50%; red >50%

Element	%CVav	Element	%CVav
Ag	36.14%	Ni	22.01%
Al	23.50%	P	16.90%
As	64.14%	Pb	18.41%
Au	70.50%	Rb	31.66%
Bi	46.39%	Re	52.77%
Ca	22.49%	S	37.57%
Cd	48.10%	Sb	26.75%
Ce	29.34%	Sc	31.31%
Co	35.58%	Se	51.87%
Cr	22.49%	Sn	28.44%
Cs	27.76%	Sr	20.63%
Cu	33.59%	Te	50.57%
Fe	26.72%	Th	46.61%
Hg	28.16%	Ti	28.44%
K	20.84%	Tl	50.98%
La	27.04%	U	40.79%
Li	43.71%	V	30.06%
Mg	24.87%	W	23.57%
Mn	56.16%	Y	32.98%
Mo	32.52%	Zn	32.29%
Na	26.90%	Zr	40.67%
Nb	30.05%		

Table 3. Summary statistics for control LKSD-4 reference material from both campaigns

Element	Units	D.L.	Average	Std. Dev.	RSD%	Element	Units	D.L.	Average	Std. Dev.	RSD%
Ag	ppb	2	255	39	15	Na	%	0.001	0.015	0.002	14
Al	%	0.01	1.19	0.04	3	Nb	ppm	0.02	1.18	0.058	5
As	ppm	0.1	14.1	0.8	6	Ni	ppm	0.1	32	2.1	7
Au	ppb	0.2	1.9	0.7	38	P	%	0.001	0.12	0.007	6
B	ppm	20	<DL			Pb	ppm	0.01	96	3.9	4
Ba	ppm	0.5	140	6	4	Pd	ppb	10	<DL		
Be	ppm	0.1	0.43	0.098	23	Pt	ppb	2	<DL		
Bi	ppm	0.02	0.52	0.045	9	Rb	ppm	0.1	9.7	0.51	5
Ca	%	0.01	0.85	0.036	4	Re	ppb	1	3.9	1.8	47
Cd	ppm	0.01	2.13	0.12	5	S	%	0.02	0.95	0.04	4
Ce	ppm	0.1	40	2.0	5	Sb	ppm	0.02	0.99	0.05	5
Co	ppm	0.1	9.3	0.56	6	Sc	ppm	0.1	3.2	0.3	9
Cr	ppm	0.5	19	1.7	9	Se	ppm	0.1	2.3	0.2	11
Cs	ppm	0.02	0.98	0.06	7	Sn	ppm	0.1	3.5	0.2	6
Cu	ppm	0.01	31	1.2	4	Sr	ppm	0.5	41	2.6	6
Fe	%	0.01	2.4	0.087	4	Ta	ppm	0.05	<DL		
Ga	ppm	0.1	4.0	0.23	6	Te	ppm	0.02	0.12	0.058	48
Ge	ppm	0.1	<DL			Th	ppm	0.1	1.3	0.16	12
Hf	ppm	0.02	0.028	0.004	14	Ti	%	0.001	0.046	0.003	7
Hg	ppb	5	186	15	8	Tl	ppm	0.02	0.39	0.021	5
In	ppm	0.02	0.05	0.013	27	U	ppm	0.05	30.6	1.1	4
K	%	0.01	0.10	0.007	7	V	ppm	2	30	1.1	4
La	ppm	0.5	21.6	1.5	7	W	ppm	0.05	0.20	0.012	6
Li	ppm	0.1	9.0	0.57	6	Y	ppm	0.01	16.7	0.78	5
Mg	%	0.01	0.35	0.02	4	Zn	ppm	0.1	187	11	6
Mn	ppm	1	420	12	3	Zr	ppm	0.1	1.3	0.10	8
Mo	ppm	0.01	1.60	0.17	11						

Spruce Sap

Total measurement errors for spruce sap duplicates are shown in Table 4. Compared to the Ah horizon, the saps exhibit much larger overall measurement errors with many elements having values of well over 50%. Lead, with a measurement error of > 100%, is noteworthy. Measurement errors of this magnitude suggest that the results are, for all intents and purposes, random numbers that are not fit for interpretation. Furthermore, several of the porphyry pathfinder elements including Ag, As, Cu and Sb also have measurement errors well above 50%. Results of these elements should be viewed with care as within site concentration differences may be sufficiently large to mask geologically meaningful patterns.

Other porphyry pathfinders like Mo, Cs, Hg, K, La, Te, W and Zn have measurement errors within acceptable limits, making them suitable for interpretation.

Large measurement errors in the field duplicate samples suggest that there are inherent differences in the concentrations of certain elements in the saps of individual trees at a sample location. These differences are caused by a combination of within site variability, the complexity of the sample medium, and the low concentrations of many elements. It implies that composite sampling of multiple trees, which was not done for this project, may have been advantageous to reduce the error levels.

Table 4. Total measurement errors for spruce sap field duplicates (n=12): Red –poor quality; gold – marginal quality; blue – acceptable quality

Element	%CVav	Element	%CVav
Ag	69.00%	Pb	71.51%
Al	71.07%	Rb	46.11%
As	72.54%	Re	43.43%
Au	51.71%	Sb	91.19%
Ba	83.67%	Se	106.12%
Be	32.14%	Sn	35.48%
Bi	53.43%	Sr	45.81%
Ca	47.85%	Te	ns
Cd	46.17%	Th	54.50%
Ce	32.89%	Ti	57.10%
Co	36.87%	Tl	80.83%
Cr	45.59%	U	57.69%
Cs	63.53%	V	50.78%
Cu	65.93%	W	36.56%
Fe	72.20%	Y	52.54%
Ga	24.71%	Zn	53.48%
Hf	41.19%	Zr	63.82%
Hg	29.44%	Pr	42.13.%
In	32.71%	Nd	40.10%
K	45.66%	Sm	25.66%
La	37.55%	Eu	44.58%
Li	62.01%	Gd	57.35%
Mg	48.05%	Tb	27.80%
Mn	50.35%	Dy	34.79%
Mo*	40.36%	Ho	38.71%
Na	20.83%	Er	40.28%
Nb	65.65%	Tm	51.31%
Ni	79.87%	Yb	56.12%
P	28.42%	Lu	95.98%

* Suspect duplicate omitted
ns - insufficient data

For Mo, once a single sample pair with extreme differences was removed, the reproducibility was very good for the remainder of the field duplicate pairs.

RESULTS

Soil pH

There is a growing body of evidence to indicate that variations in soil pH, or hydrogen ion (H^+) activity, occur at the surface over buried sulphide mineralization. Smee (1983) proposed a mechanism, based on laboratory experiments and field tests, for the formation of metal anomalies in soils developed on glaciolacustrine clays over massive sulphides in the Abitibi Belt, northern Quebec. His work showed that H^+ released as a byproduct of sulphide oxidation at the water table diffuses to the surface to form detectable acidic anomalies.

More recent work by Hamilton *et al*. (2004 a, b) at the Marsh zone gold prospect and the Cross Lake volcanogenic massive sulphide (VMS) prospect in Ontario, shows that "rabbit-ear" patterns occur in H^+ at the surface, over the edges of blind or buried sulphide mineralization. They conclude that pH correlates

with oxidation-reduction potential (ORP) and propose that H^+ production is a function of changes in the redox conditions of the overburden column in response to sulphide oxidation.

At the regional scale, soil pH variations are expected to highlight expressions of oxidizing sulphides within the hydrothermal alteration system related to mineralization. Zones of increased acidity, manifest as higher H^+ ion activities, can be expected to occur over areas with higher than background sulphide contents.

Results for H^+ are shown in Figure 9. Hydrogen ion concentrations are highest (indicating acid conditions) in the vicinity of the Endako mine. Values substantially higher than background surround the ore body (red outline) and extend for distances of up to 1.2 km to the northwest, 3.4 km to the east and 1.6 km to the south of the deposit. Highest values occur peripheral to a K radiometric anomaly (Devine *et al.,* in press) that defines the extent of potassic alteration. The halo of high H^+ values is interpreted to indicate the extent of the pyrite halo around the margins of porphyry Mo system and not to be significantly affected by anthropogenic factors.

At Nithi Mountain, where low grade Mo mineralization also occurs (Mosher, 2011), the soil H^+ response is less convincing. Only scattered moderately anomalous values are present on the northern and southern flanks of the mountain. The highest value lies in the vicinity of the Gamma West zone (Mosher, 2011). The weak response could be due to a combination of the relatively small size of the mineralized system and the coarse sample spacing in that part of the survey area.

Another prominent response is identified over Skeena Group rocks in the southwest part of the survey area, south of François Lake. This feature is defined by two highly anomalous samples. There are no known mineral occurrences in this area to explain these anomalous readings.

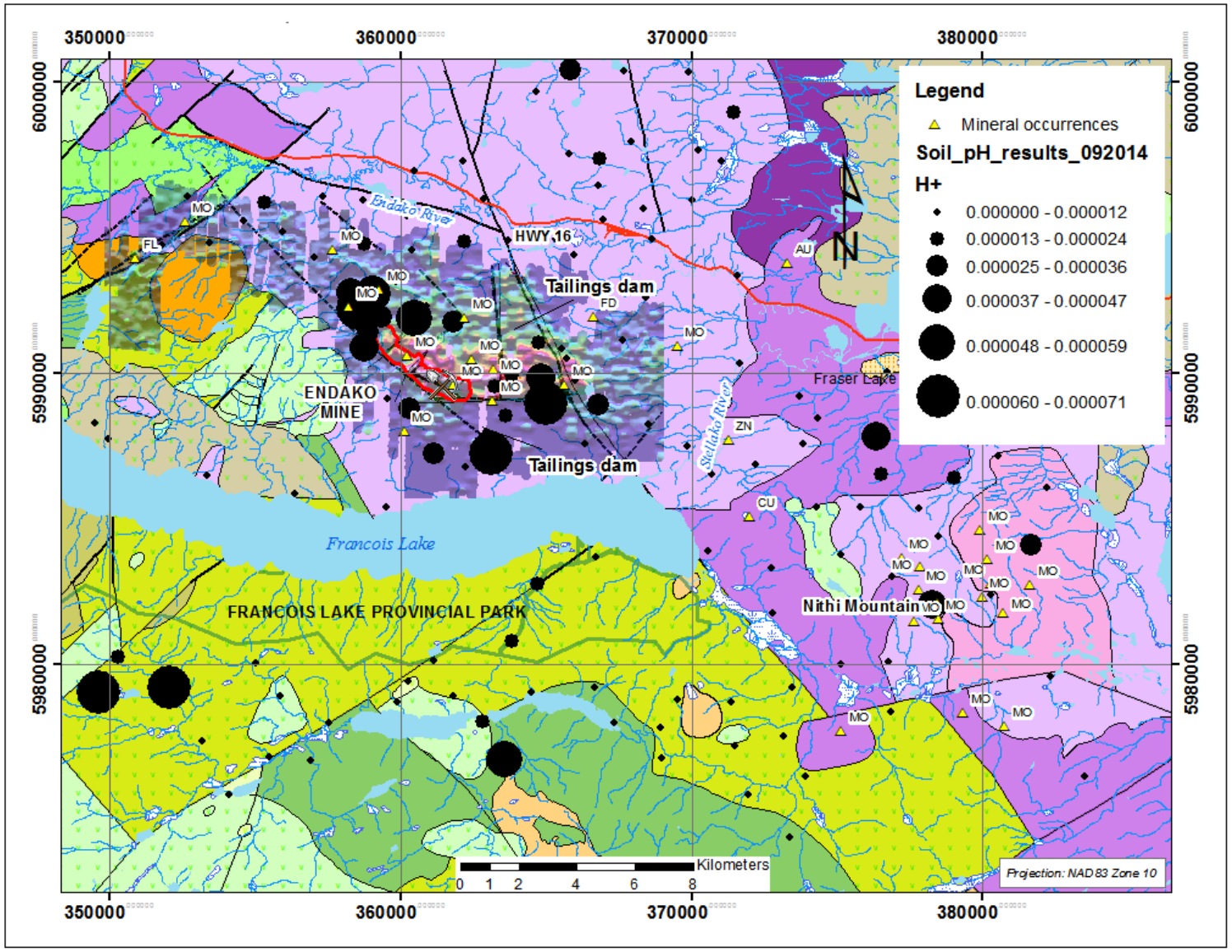

Figure 9. Soil pH results showing H^+ distribution Ah Horizon superimposed on gridded data from analysis of B-horizon soils (from Devine et al., in press) .

Ah Horizon

Table 5 shows some summary statistics for the Ah soil horizon results.

Table 5. Summary Statistics for Ah horizon samples

Element	N	Min*	Max	Range	Mean	Median	St Dev	CV%	IQR
Ag_ppb	137	16	3708	3692	258.32	161	358.855	138.918	208.5
Al_pct	137	0.11	4.19	4.08	0.69	0.56	0.583	84.492	0.42
As_ppm	137	0.05	21.9	21.85	1.42	1	2.071	146.101	1.15
Au_ppb	137	0.1	4.4	4.3	0.45	0.1	0.684	151.941	0.45
B_ppm	137	10	10	0	10.00	10	0.000	0.000	0
Ba_ppm	137	30.8	961.5	930.7	225.64	190.4	140.124	62.100	178.9
Be_ppm	137	0.05	3.5	3.45	0.35	0.2	0.471	136.543	0.3
Bi_ppm	137	0.01	2.11	2.1	0.22	0.11	0.291	133.812	0.185
Ca_pct	137	0.12	3.27	3.15	0.86	0.74	0.567	66.081	0.72
Cd_ppm	137	0.005	4.66	4.655	0.57	0.39	0.626	110.326	0.41
Ce_ppm	137	2.1	517.4	515.3	24.35	13.7	49.256	202.262	11.85
Co_ppm	137	0.6	17.3	16.7	4.53	4.3	2.768	61.087	2.95
Cr_ppm	137	2.7	43.9	41.2	9.69	9.1	5.385	55.550	5.85
Cs_ppm	137	0.1	11.22	11.12	1.10	0.51	1.724	157.191	0.625
Cu_ppm	137	2.13	82.2	80.07	12.90	9.2	12.065	93.551	9.025
Fe_pct	137	0.19	3.52	3.33	1.21	1.14	0.601	49.694	0.75
Ga_ppm	137	0.4	11.5	11.1	2.64	2.4	1.552	58.787	1.35
Ge_ppm	137	0.05	0.3	0.25	0.05	0.05	0.022	41.677	0
Hf_ppm	137	0.01	0.22	0.21	0.02	0.01	0.030	122.999	0.02
Hg_ppb	137	25	263	238	93.63	89	45.842	48.962	55.5
In_ppm	137	0.01	0.08	0.07	0.01	0.01	0.010	76.646	0
K_pct	137	0.02	0.31	0.29	0.10	0.08	0.051	53.882	0.05
La_ppm	137	1.2	307.2	306	15.27	7.2	34.693	227.239	6.15
Li_ppm	137	0.3	31.5	31.2	4.24	3.3	4.424	104.315	3.35
Mg_pct	137	0.02	0.67	0.65	0.19	0.18	0.112	59.688	0.15
Mn_ppm	137	50	8056	8006	1263.98	1020	1183.463	93.630	1151

Element	N	Min*	Max	Range	Mean	Median	St Dev	CV%	IQR
Na_pct	137	0.003	0.069	0.066	0.008	0.006	0.007	92.404	0.003
Nb_ppm	137	0.06	1.8	1.74	0.474	0.43	0.253	53.338	0.22
Ni_ppm	137	1.3	36.3	35	7.587	7	5.482	72.256	5.6
P_pct	137	0.02	0.237	0.217	0.089	0.086	0.039	43.443	0.0505
Pb_ppm	137	2.64	41.29	38.65	8.276	7.06	4.940	59.694	3.225
Pd_ppb	137	0	50	50	6.993	5	8.243	117.881	0
Pt_ppb	137	1	3	2	1.073	1	0.335	31.229	0
Rb_ppm	137	0.6	31.8	31.2	7.266	5.8	5.121	70.471	4.95
Re_ppb	137	0.5	130	129.5	6.974	2	17.220	246.907	4
S_pct	137	0.01	0.32	0.31	0.056	0.05	0.040	71.757	0.04
Sb_ppm	137	0.05	0.6	0.55	0.164	0.14	0.094	57.203	0.07
Sc_ppm	137	0.2	11.6	11.4	1.501	1.2	1.467	97.708	1.05
Se_ppm	137	0.05	2.1	2.05	0.180	0.1	0.245	136.521	0.15
Sn_ppm	137	0.05	1.7	1.65	0.327	0.3	0.228	69.744	0.15
Sr_ppm	137	13	359.2	346.2	90.420	77	57.593	63.694	62.9
Ta_ppm	137	0.025	0.025	0	0.025	0.025	0.000	0.000	0
Te_ppm	137	0.01	0.17	0.16	0.026	0.01	0.026	99.256	0.03
Th_ppm	137	0.05	5.3	5.25	0.468	0.2	0.826	176.407	0.4
Ti_pct	137	0.004	0.059	0.055	0.024	0.024	0.012	49.364	0.017
Tl_ppm	137	0.01	0.4	0.39	0.052	0.03	0.061	118.666	0.035
U_ppm	137	0.05	111.18	111.13	1.994	0.3	10.399	521.419	0.4
V_ppm	137	2	56	54	24.255	24	10.789	44.483	15.5
W_ppm	137	0.025	1.5	1.475	0.097	0.05	0.136	140.113	0.05
Y_ppm	137	0.45	132.63	132.18	7.508	2.62	16.818	223.989	2.92
Zn_ppm	137	11	624.4	613.4	82.235	62.4	73.097	88.888	67.45
Zr_ppm	137	0.05	6.6	6.55	0.847	0.6	1.014	119.702	0.7

* Minimum values are equivalent to half the detection limit for some elements

The element distribution plots (Figs. 10 to 12) each have proportional dots sized according to the <50th, 75th, 87th, 93rd, 96th and >98th percentiles They show those elements that best define the Endako mineralization, arranged in a sequence of approximate decreasing response to mineralization: Mo, Re, Bi, W, S, Se, Te, Sn, Tl, Pb, Cs and Rb.

Highest concentrations of Mo, Re and Bi occur to the east and south of the Endako mine site (Fig. 10a, b, c). This pattern is consistent with historical soil results (Fig. 11) that show anomalous values extending some 6 km east of the mine. This elongation is parallel to the regional ice-flow-direction and therefore could be the result of down-ice glacial dispersal of mineralized material. However, Mo occurrences within the soil anomaly suggest that at least part of the pattern may be in situ. This distribution is mimicked by Re (Fig. 10b). Neither element is anomalous over Nithi Mountain.

High Bi and W values occur around the edges of the Endako mine site (Fig. 10c and d). Anomalous levels of Bi cluster to the east, north and south of the mine. Tungsten patterns define a more continuous halo with higher concentrations developed east of the deposit and an isolated occurrence to the northwest as well as a focused anomaly over the Gamma and Gamma West zones (Mosher, 2011; Fig. 9). Elevated concentrations of these elements also occur in the Nithi Mountain area. Both Bi and W are sporadically enriched over Skeena Group rocks south of François Lake.

Figures 12a to d shows the results for Sn, Se, Te and S. Tin (Fig. 12a) has a similar distribution to Bi and W. Highest concentrations lie immediately to the east of the Endako mine with sporadic highs also present on the north and northwest sides. Like Bi and W, Sn also displays anomalous values over the Skeena Group south of François Lake. Selenium and Te (Fig. 12 b and c) are moderately elevated close to Endako, again with highest concentrations on the east side. Tellurium (Fig. 12c) also shows an elevated response at Nithi Mountain and defines a cluster of anomalous samples centred on the northern margin of the Sam Ross Creek pluton in the northwest part of the study area (orange; Fig. 12).

Sulphur patterns (Fig. 12d) are less compelling. There is a general enrichment close to the Endako Mine but scattered anomalous values also occur throughout the François Lake Suite of the Endako Batholith north of the mine (pale mauve; Fig. 12). Isolated high S values are also scattered over the Skeena Group exposures south of François Lake.

Figure 13 shows elements that have highest concentrations mostly over the Skeena Group south of François Lake (especially Tl and Cs), with Rb (Fig. 13b) having concentrations of similar magnitude around Endako. Lead (Fig. 13d) has scattered values that are elevated peripherally to the Endako mineralization.

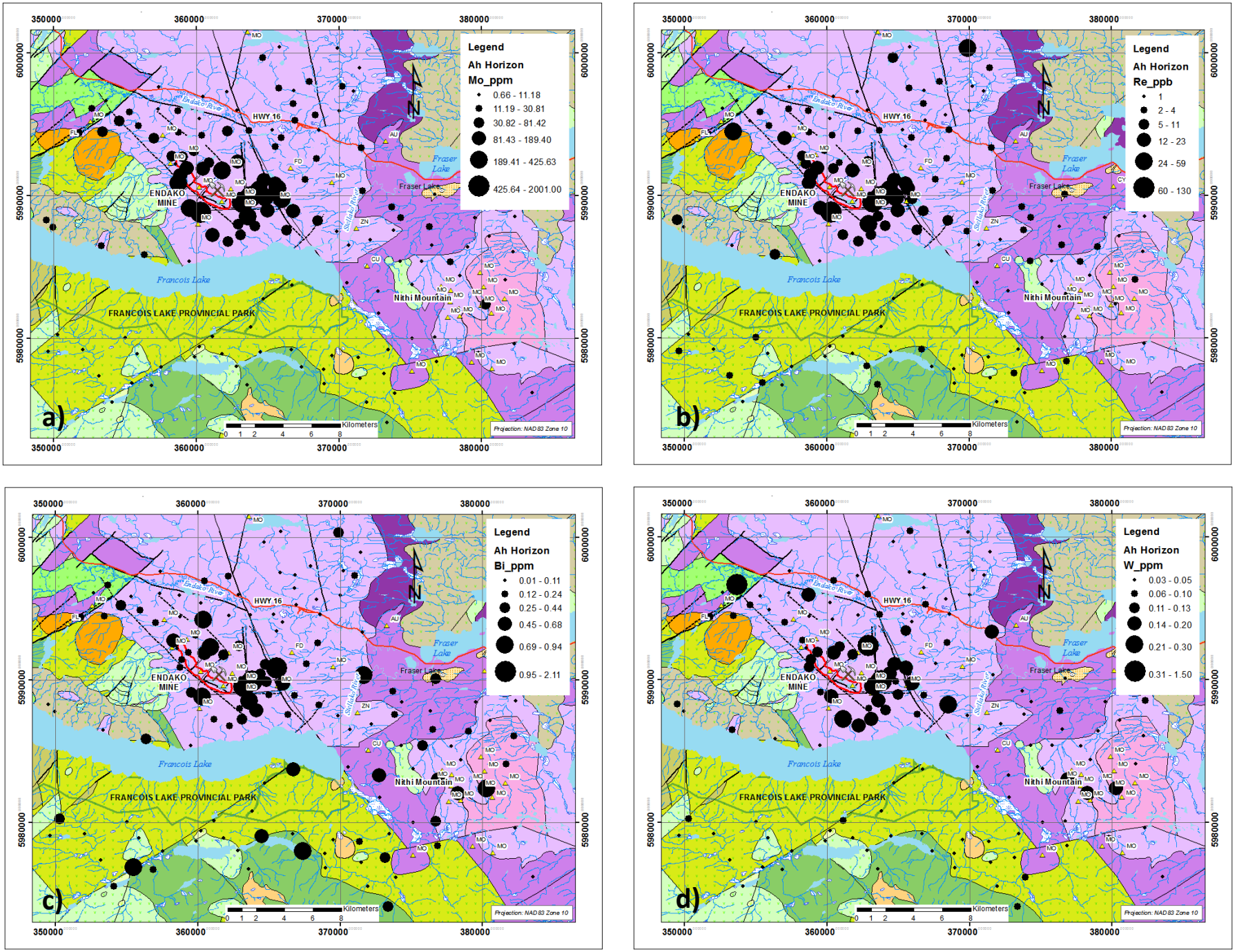

Figure 10. Molybdenum, Re, Bi and W in Ah horizon soil. Endako orebody is indicated by the red outline.

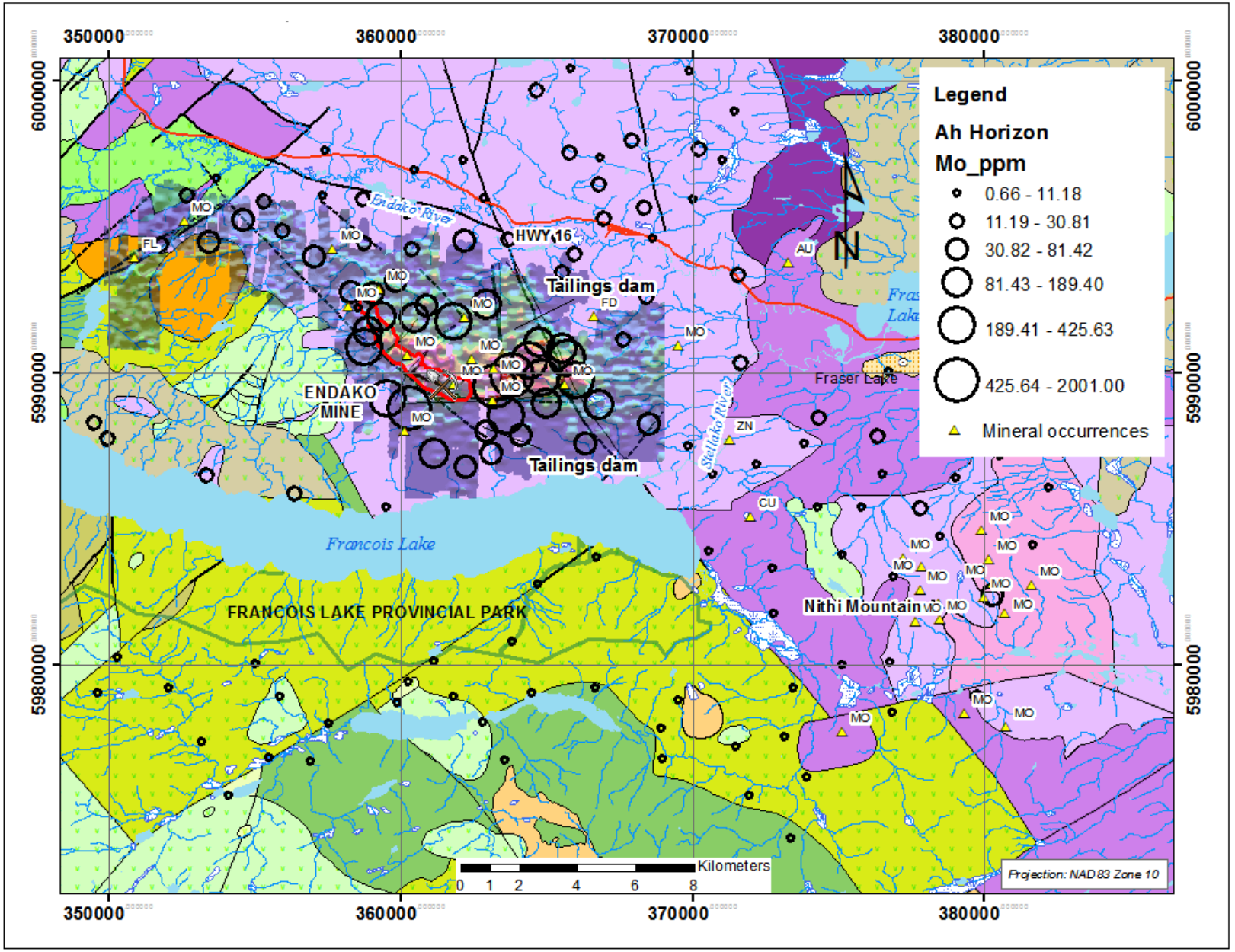

Figure 11. Concentrations of Mo in Ah (this study) and historical B horizon soils shown as gradational colours around Endako (Devine et al., in press).

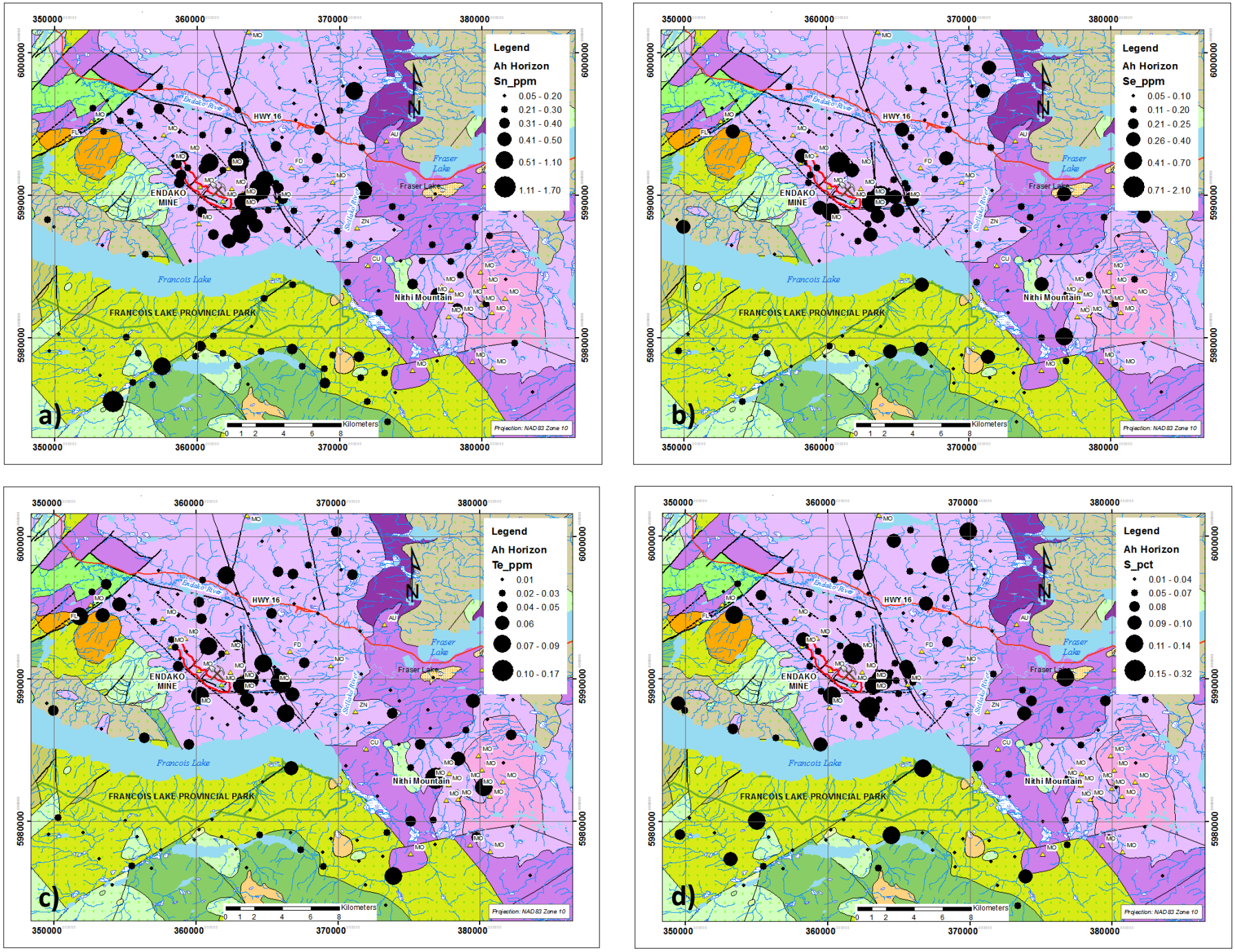

Figure 12. Tin, Se, Te, S in Ah horizon soil. Endako orebody is indicated by the red outline.

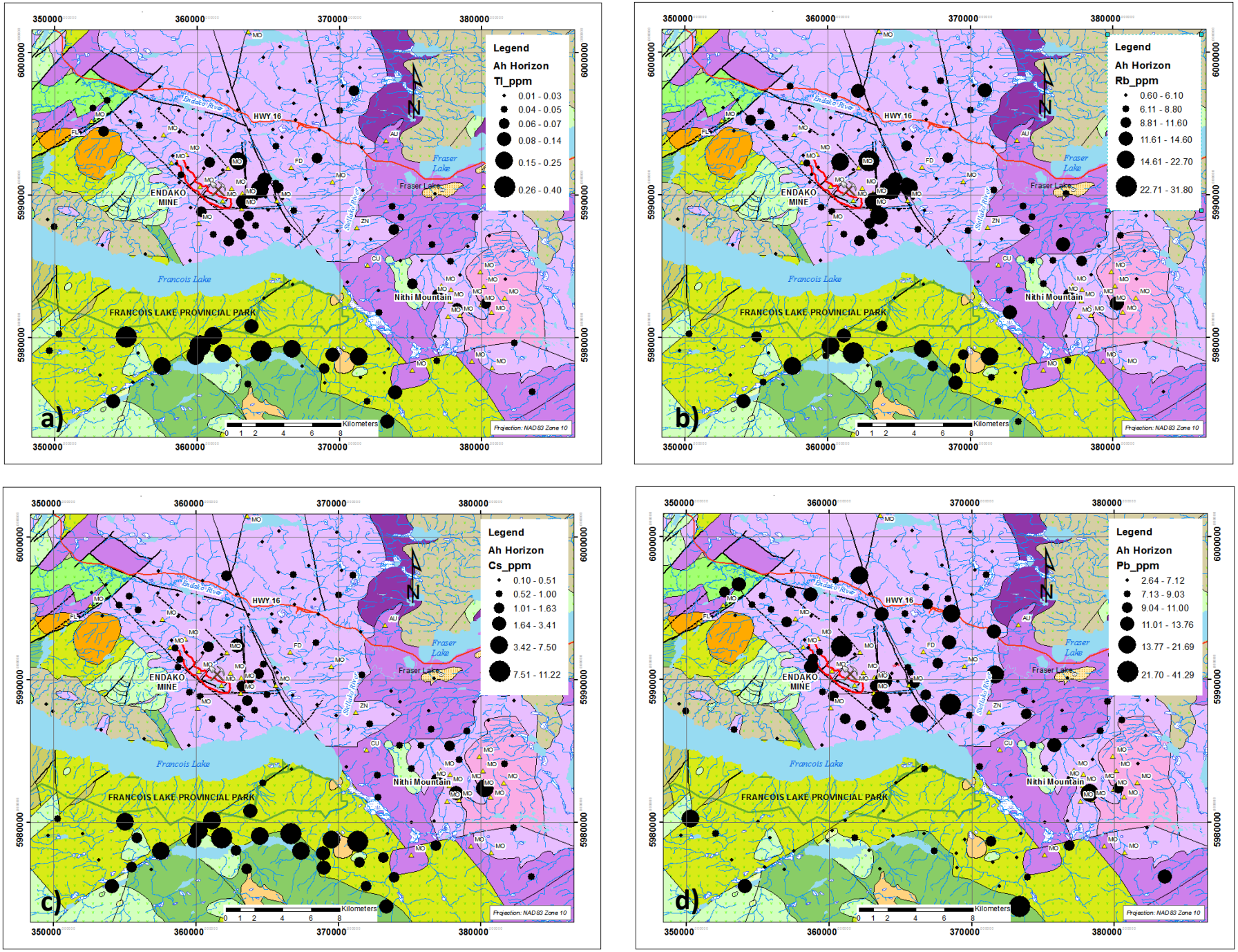

Figure 13. Thallium, Rb, Cs and Pb in Ah horizon soil. Endako orebody is indicated by the red outline.

Spruce Sap

Element distribution patterns in spruce sap.

As might be expected, and consistent with the Ah and B horizon soils, the element that exhibits the most pronounced concentrations in the vicinity of the Endako mine is Mo (Fig. 14a). The background concentration (expressed as the median) is 178 ppb Mo, whereas around the Endako mine concentrations are up to almost 50 times background (8,463 ppb Mo). Elsewhere in the survey area there are some isolated sites with concentrations more than an order of magnitude above background, especially at sites on the Skeena Group rocks south of François Lake Provincial Park (no samples were taken from within the park), and over other phases of the Endako batholith. No sites have strongly elevated Mo levels near any of the Mo occurrences in the Nithi Phase, east of Nithi Mountain.

Rhenium (Fig. 14b) shows enrichments around the Endako mine and south of Nithi Mountain, but with less contrast (an order of magnitude above background) than Mo. There is a moderately good spatial relationship between Mo and Re, but the Re is less well-defined.

Bismuth (Fig. 14c) is up to 7 times background at Endako, whereas the contrast in U (Fig. 15d) is much higher and similar to Mo (more than 50 times background).

Plots of Th and some REE are shown in Figure 15, with La, Dy and Nd taken as typical examples of REE. These elements each have maximum values that are approximately 25 times background. Their distribution patterns are all very similar. Of note is that some anomalous values are spatially related to NW-trending faults through the Endako batholith.

Figure 16 shows that K and Rb are somewhat depleted around the Endako mine site, whereas Ag is enriched up to 6 times background to the south and east of the mine; Cs, also 6 times background, tends to follow the northwest-trending faults. Both Cs and Rb are moderately enriched over Skeena Group south of François Lake. Potassium is enriched (up to 3-fold) at some of these same sites.

Manganese (Fig. 17) is enriched 12-fold at the mine site, along NW-trending faults, and close to a northeast-trending fault that cuts the Skeena Group rocks south of François Lake. Sodium and P are depleted at Endako, but are more enriched to the north and east. Strontium is relatively enriched over the Skeena Group to the south.

c)

d)

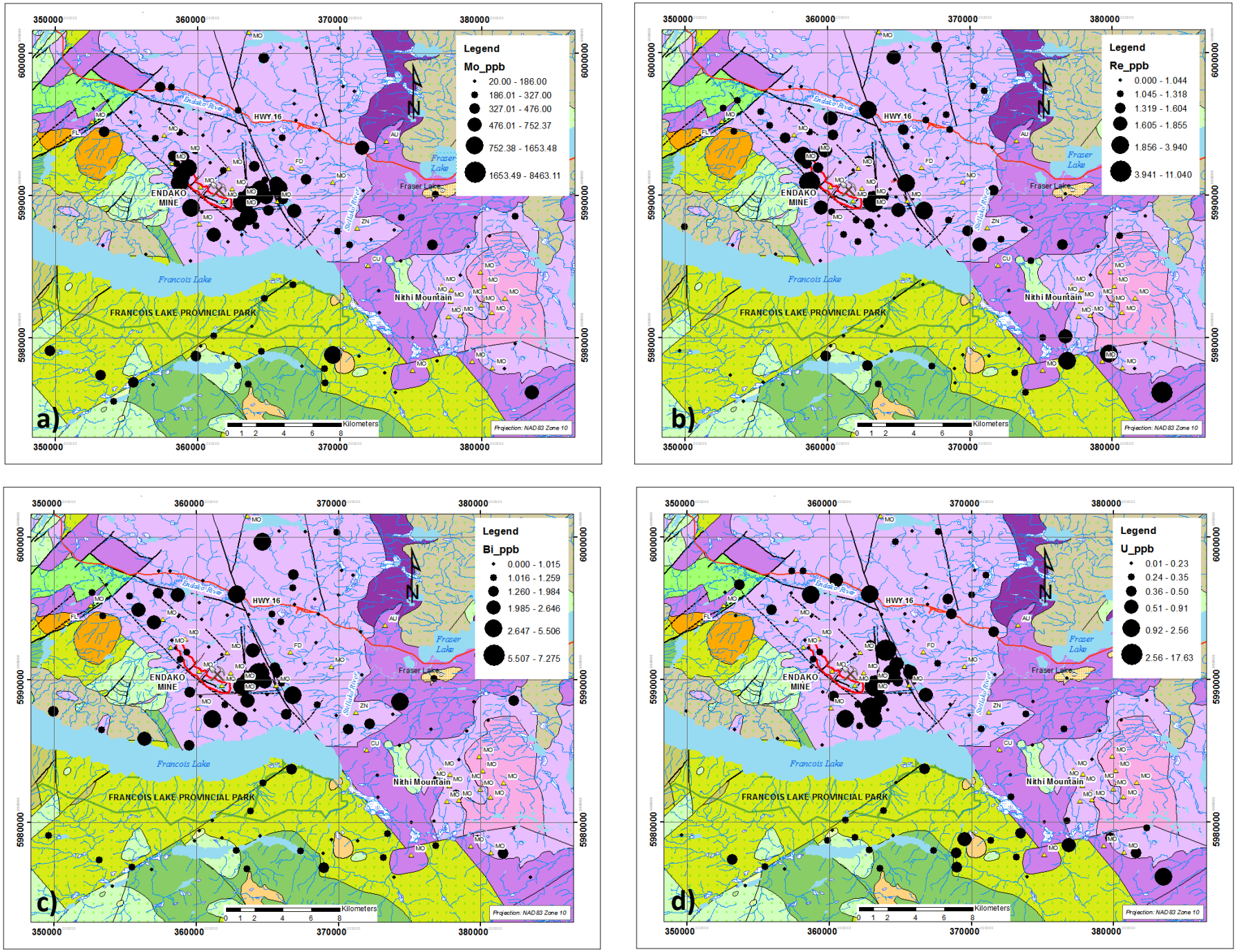

Figure 14 Molybdenum, Re, Bi and U in spruce sap. Endako orebody is indicated by the red outline.

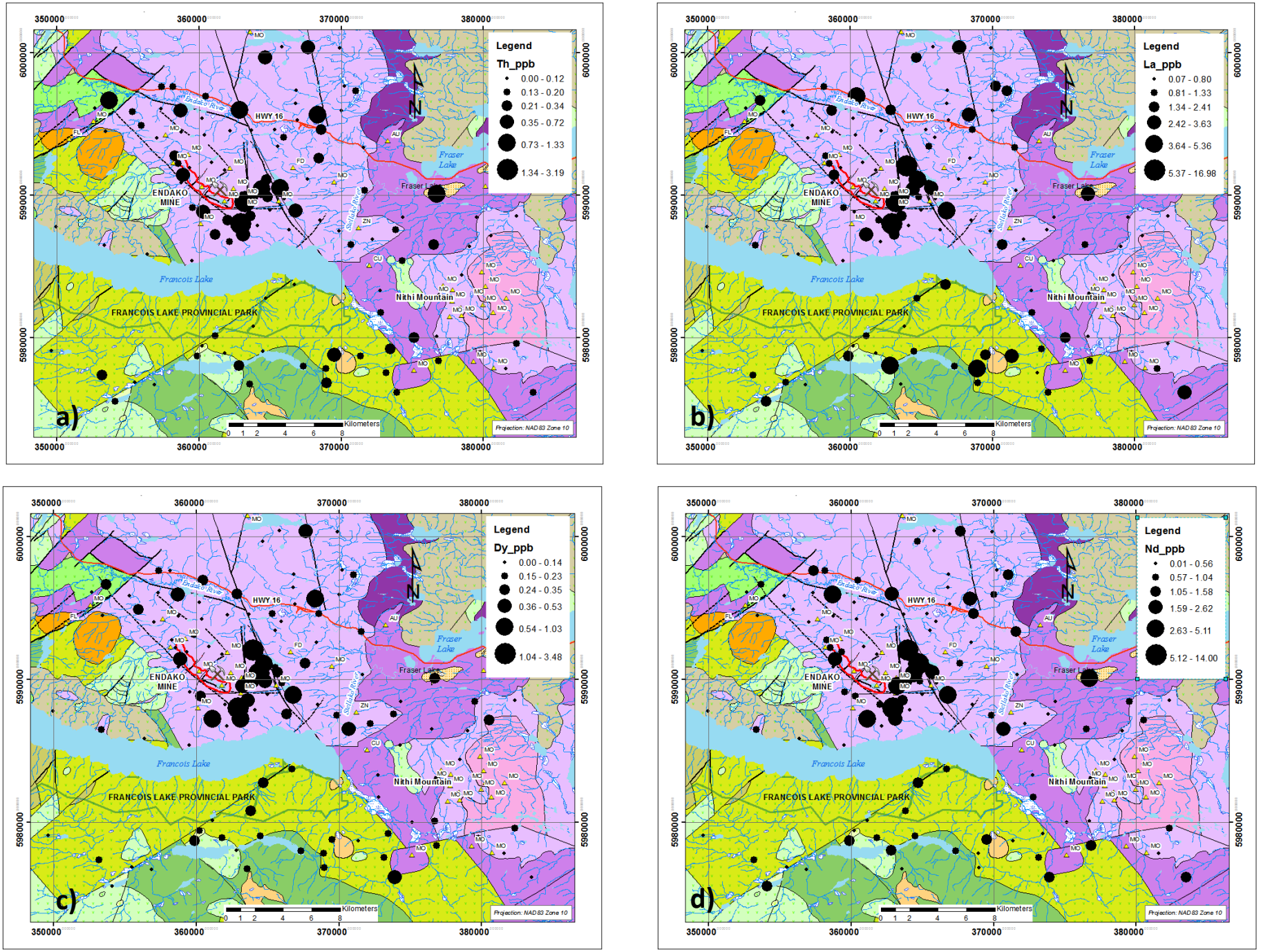

Figure 15. Thorium, La, Dy and Nd in spruce sap. Endako orebody is indicated by the red outline.

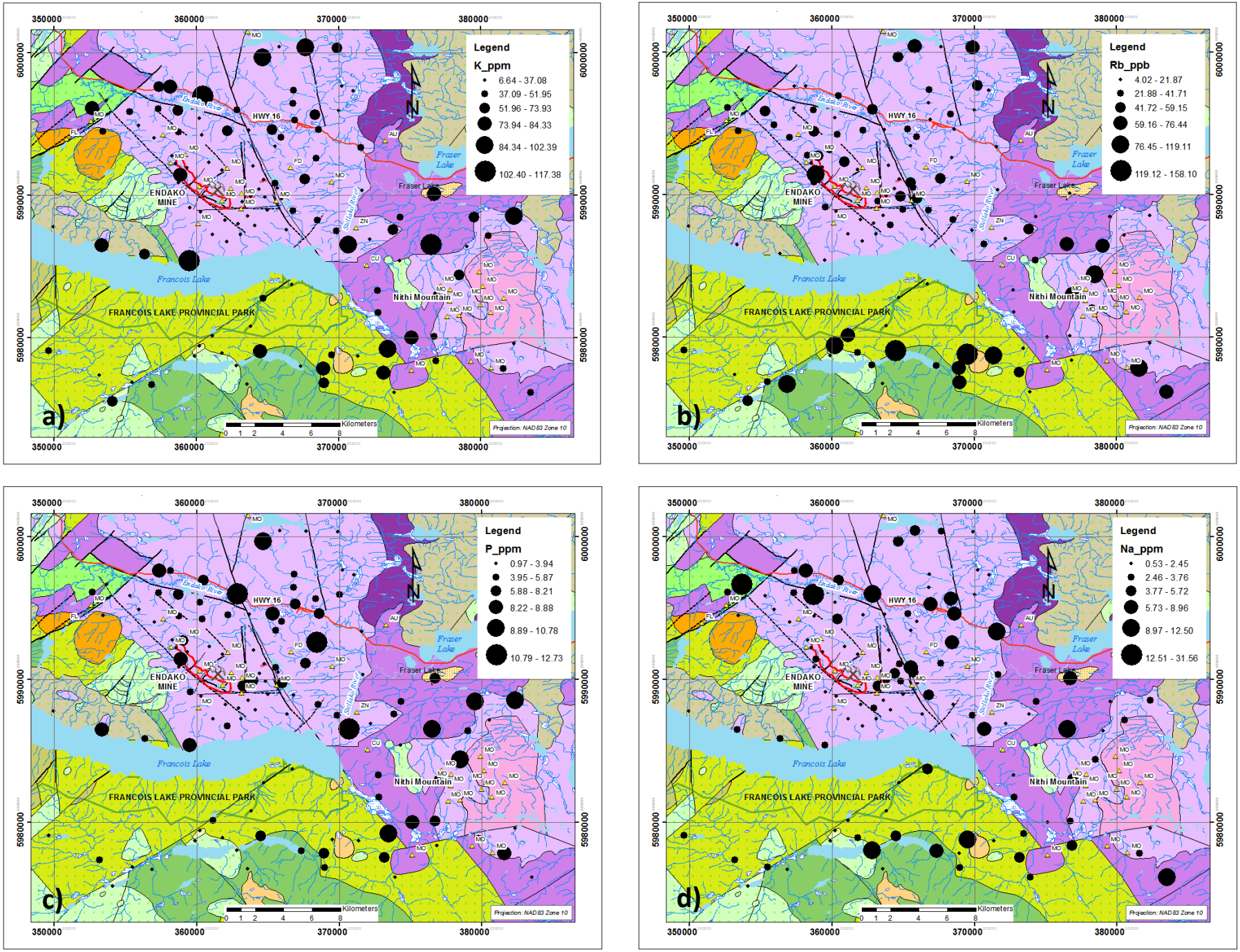

Figure 16. Potassium, Rb, P and Na in spruce sap. Endako orebody is indicated by the red outline.

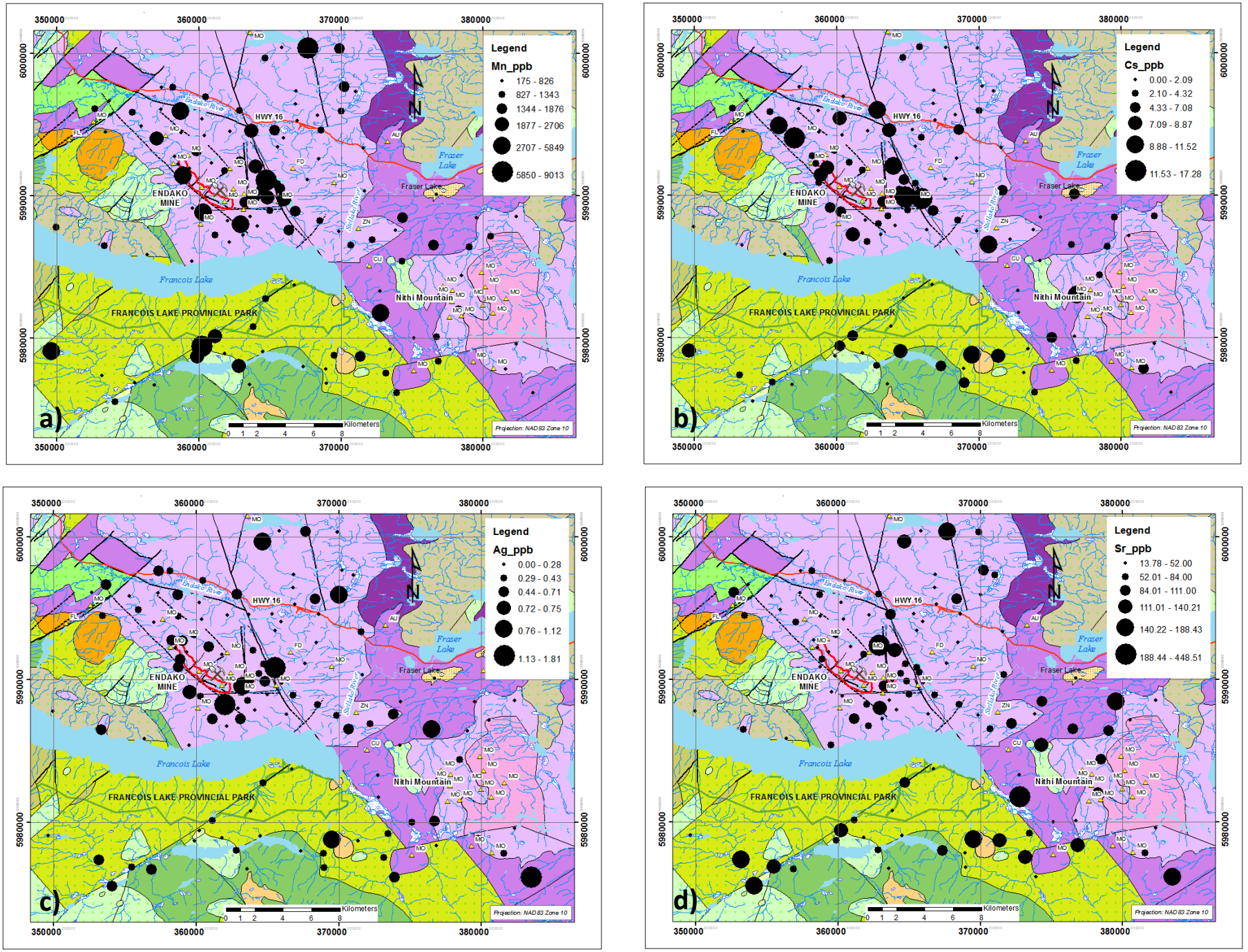

Figure 17. Manganese, Cs, Ag and Sr in spruce sap. Endako orebody is indicated by the red outline.

Comparisons of spruce and lodgepole pine sap

Table 6 lists some basic summary statistics of the white spruce sap results and shows that there are wide ranges in concentration for most elements, most notably Mo, Pb, Cu, Ni and Zn as indicated by their high interquartile ranges (IQR).

Table 7 lists the same statistical parameters for the 12 pine saps, and shows a similar wide range in concentrations of the same elements as in the spruce.

Table 6. Summary statistics for spruce sap results (refer to Table 4 for data quality)

Element	N	Min	Max	Range	Mean	Median	St. Dev	CV%	IQR
Ag_ppb	119	0.019	1.81	1.79	0.35	0.29	0.29	83.80	0.28
Al_ppm	118	1.043	43.50	42.46	10.82	8.20	8.56	79.07	8.11
As_ppb	120	0.109	38.54	38.43	9.13	7.65	6.21	67.96	8.24
Au_ppb	118	0.022	1.25	1.23	0.43	0.34	0.28	64.86	0.40
B_ppb	117	141.340	11356.69	11215.35	4197.47	4077.11	2802.35	66.76	4485.43
Ba_ppb	120	2.082	571.07	568.99	80.68	44.10	98.73	122.36	84.31
Be_ppb	119	0.011	2.44	2.43	0.30	0.25	0.31	101.07	0.25
Bi_ppb	119	0.033	7.27	7.24	1.33	1.02	1.04	78.25	0.37
Ca_ppb	120	1.657	80.14	78.49	12.49	9.23	10.97	87.81	8.33
Cd_ppb	120	0.025	37.32	37.29	4.37	2.79	5.13	117.49	3.90
Ce_ppb	120	0.076	25.91	25.83	2.47	1.40	3.67	148.75	2.00
Co_ppb	119	1.303	20.16	18.85	5.23	4.48	3.19	60.86	2.48
Cr_ppb	119	28.757	6715.69	6686.93	1962.60	1800.00	1286.41	65.55	1435.91
Cs_ppb	105	0.052	17.28	17.23	3.63	2.54	3.30	90.82	3.53
Cu_ppb	120	3.119	624.89	621.77	85.64	52.30	99.52	116.20	65.37
Dy_ppb	119	0.007	3.48	3.47	0.24	0.14	0.45	187.20	0.16
Er_ppb	118	0.000	2.26	2.26	0.16	0.10	0.29	178.65	0.08
Eu_ppb	119	0.003	0.81	0.81	0.08	0.05	0.10	128.26	0.06
Fe_ppm	120	0.047	46.05	46.00	2.91	1.09	6.24	213.97	1.91
Ga_ppb	120	0.006	19.73	19.72	5.89	5.40	2.44	41.38	2.39
Gd_ppb	119	0.002	3.32	3.32	0.26	0.17	0.41	159.67	0.16
Ge_ppb	113	0.015	4.49	4.48	0.78	0.54	0.67	86.65	0.52
Hf_ppb	119	0.012	0.96	0.94	0.16	0.13	0.14	86.17	0.12
Hg_ppb	119	0.417	3.50	3.08	1.90	1.89	0.59	31.26	0.79
Ho_ppb	120	0.005	0.76	0.76	0.06	0.04	0.10	154.38	0.04
In_ppb	119	0.012	1.44	1.43	0.20	0.17	0.16	84.15	0.09
K_ppb	120	6.640	117.38	110.74	41.83	37.13	23.56	56.32	27.10
La_ppb	120	0.071	16.98	16.91	1.43	0.80	2.18	152.87	1.01
Li_ppb	119	0.004	79.32	79.31	6.54	4.28	9.51	145.30	4.01
Lu_ppb	120	0.000	0.34	0.34	0.06	0.04	0.06	99.95	0.06
Mg_ppm	120	0.691	12.24	11.55	3.09	2.66	1.67	54.06	1.74
Mn_ppb	120	175.031	9012.60	8837.57	1216.42	828.15	1280.02	105.23	893.79
Mo_ppb	120	20.000	8463.11	8443.11	378.19	178.17	864.52	228.59	199.44
Na_ppm	120	0.528	31.56	31.03	3.61	2.45	3.90	108.06	1.94
Nb_ppb	118	0.000	1.47	1.47	0.37	0.30	0.29	77.34	0.37
Nd_ppb	120	0.014	14.00	13.99	1.07	0.57	1.80	168.10	0.76
Ni_ppb	120	0.432	259.23	258.80	50.84	39.32	46.01	90.48	40.55
P_ppm	120	0.970	12.73	11.76	4.55	3.98	2.59	56.90	3.41
Pb_ppb	106	0.104	240.06	239.96	16.59	7.87	32.76	197.45	10.38
Pd_ppb	105	0.000	0.83	0.83	0.16	0.11	0.15	94.55	0.19
Pr_ppb	120	0.007	3.51	3.50	0.26	0.15	0.43	164.42	0.16
Pt_ppb	119	0.018	1.30	1.28	0.43	0.36	0.25	59.30	0.34
Rb_ppb	120	4.025	158.10	154.08	32.67	22.76	28.61	87.55	28.01
Re_ppb	119	0.009	11.04	11.03	1.15	1.05	1.14	98.68	0.62
Sb_ppb	113	0.005	9.47	9.47	1.34	1.07	1.25	93.35	1.31
Se_ppb	114	2.000	33.24	31.24	6.34	5.18	5.48	86.56	5.67
Sm_ppb	118	0.003	3.62	3.62	0.30	0.19	0.42	143.12	0.24
Sn_ppb	120	16.524	407.67	391.14	83.05	71.46	60.10	72.37	55.47
Sr_ppb	120	13.778	448.51	434.73	67.10	52.41	57.90	86.28	50.98
Ta_ppb	119	0.002	3.12	3.12	0.11	0.06	0.29	259.49	0.08
Tb_ppb	120	0.000	0.60	0.60	0.05	0.03	0.08	170.51	0.03
Te_ppb	80	0.034	8.67	8.64	1.42	0.81	1.29	90.54	0.90
Th_ppb	119	0.012	3.19	3.18	0.24	0.12	0.44	180.90	0.13
Ti_ppb	120	0.050	174.43	174.38	37.51	30.75	27.55	73.46	25.46
Tl_ppb	118	0.008	1.48	1.47	0.37	0.31	0.28	77.44	0.29
Tm_ppb	119	0.000	0.37	0.37	0.03	0.03	0.04	129.62	0.02
U_ppb	120	0.013	17.63	17.62	0.58	0.23	2.05	353.51	0.24
V_ppb	119	0.022	336.45	336.43	87.96	87.06	55.28	62.84	67.26
W_ppb	120	0.262	65.36	65.10	4.24	3.17	6.14	144.89	2.05
Y_ppb	120	0.007	18.80	18.80	1.08	0.56	2.44	225.69	0.69
Yb_ppb	119	0.011	2.17	0.22	2.16	0.26	0.19	0.28	108.90
Zn_ppb	120	128.370	2951.52	420.51	2823.15	807.82	671.74	562.15	69.59
Zr_ppb	119	0.157	26.77	3.47	26.62	4.99	3.57	4.40	88.11

Table 7. Summary statistics for pine sap analyses (refer to Table 4 for data quality)

Element	N	Min	Max	Range	Mean	Median	St. Dev	CV%	IQR
Ag_ppb	12	0.024	0.90	0.87	0.36	0.24	0.30	82.87	0.50
Al_ppm	12	7.965	44.41	36.44	19.46	18.98	10.27	52.77	15.30
As_ppb	12	2.720	16.83	14.11	10.40	10.49	3.57	34.35	3.40
Au_ppb	12	0.024	0.97	0.94	0.31	0.26	0.28	91.28	0.40
B_ppb	12	258.942	10927.59	10668.64	4242.15	3962.64	3605.59	84.99	5991.43
Ba_ppb	12	1.280	54.38	53.10	16.95	11.51	15.08	88.95	20.35
Be_ppb	12	0.022	0.60	0.58	0.31	0.24	0.19	60.24	0.33
Bi_ppb	12	0.435	1.45	1.02	1.00	0.97	0.28	28.36	0.44
Ca_ppm	12	5.114	40.65	35.54	11.88	9.65	9.49	79.89	5.85
Cd_ppb	12	0.715	24.44	23.72	5.89	2.84	7.90	134.16	2.32
Ce_ppb	12	0.308	7.15	6.84	2.28	1.98	1.89	82.72	2.40
Co_ppb	12	0.941	23.30	22.36	5.27	3.58	5.95	112.95	3.54
Cr_ppb	12	6.303	6028.91	6022.61	1984.59	1431.46	1793.40	90.37	2188.57
Cs_ppb	12	1.188	11.06	9.88	5.73	5.43	2.98	52.02	4.54
Cu_ppb	12	6.637	293.67	287.03	95.30	56.45	96.85	101.64	100.61
Dy_ppb	12	0.044	0.99	0.94	0.20	0.09	0.26	132.29	0.18
Er_ppb	12	0.068	0.25	0.18	0.15	0.15	0.07	44.79	0.12
Eu_ppb	12	0.017	0.16	0.14	0.06	0.06	0.04	63.35	0.05
Fe_ppm	12	0.126	7.05	6.93	2.29	1.89	2.26	98.66	2.43
Ga_ppb	12	3.450	8.48	5.03	5.71	5.37	1.58	27.72	2.06
Gd_ppb	12	0.032	0.60	0.57	0.22	0.15	0.18	84.60	0.32
Ge_ppb	12	0.024	2.02	1.99	0.89	0.82	0.55	61.67	0.57
Hf_ppb	12	0.033	0.48	0.45	0.20	0.15	0.16	79.63	0.28
Hg_ppb	12	1.083	2.31	1.23	1.62	1.56	0.37	22.56	0.49
Ho_ppb	12	0.001	0.10	0.10	0.05	0.04	0.03	66.23	0.04
In_ppb	12	0.070	0.61	0.54	0.26	0.25	0.15	56.64	0.13
K_ppm	12	10.780	42.14	31.36	19.67	14.78	10.99	55.88	9.76
La_ppb	12	0.025	3.61	3.59	1.20	1.10	0.92	76.78	0.85
Li_ppb	12	0.879	5.88	5.00	2.85	2.35	1.69	59.09	2.45
Lu_ppb	12	0.000	0.05	0.05	0.03	0.03	0.01	45.17	0.01
Mg_ppm	12	1.493	9.87	8.38	4.27	3.45	2.46	57.71	3.41
Mn_ppb	12	234.628	1881.24	1646.61	739.48	547.85	529.27	71.57	748.06

Element	N	Min	Max	Range	Mean	Median	St. Dev	CV%	IQR
Mo_ppb	12	20.000	1683.21	1663.21	324.71	163.39	472.03	145.37	211.96
Na_ppm	12	0.616	9.63	9.02	3.19	2.53	2.68	84.00	2.89
Nb_ppb	12	0.088	2.52	2.43	0.47	0.23	0.67	142.11	0.23
Nd_ppb	12	0.067	3.42	3.36	1.03	0.69	1.07	103.96	1.35
Ni_ppb	12	0.000	204.49	204.49	68.05	53.71	61.63	90.56	58.76
P_ppm	12	1.502	9.01	7.51	4.00	3.55	2.16	54.08	2.00
Pb_ppb	12	0.263	175.34	175.08	20.98	7.56	48.80	232.65	8.27
Pd_ppb	12	0.000	0.28	0.28	0.10	0.05	0.10	99.31	0.17
Pr_ppb	12	0.072	0.85	0.78	0.27	0.19	0.24	87.29	0.33
Pt_ppb	12	0.129	1.05	0.92	0.40	0.37	0.25	62.03	0.24
Rb_ppb	12	3.888	62.42	58.53	20.63	16.13	16.99	82.34	19.41
Re_ppb	12	0.002	3.31	3.31	0.84	0.65	0.95	113.61	1.27
Sb_ppb	12	0.432	5.44	5.01	1.90	1.07	1.85	97.22	2.60
Se_ppb	12	0.000	13.97	13.97	5.73	5.44	4.32	75.45	7.29
Sm_ppb	12	0.082	1.00	0.92	0.30	0.21	0.26	86.51	0.20
Sn_ppb	12	9.723	173.08	163.36	59.02	43.75	51.46	87.18	58.82
Sr_ppb	12	5.709	120.43	114.72	34.12	22.56	33.09	96.97	14.16
Ta_ppb	12	0.008	0.15	0.14	0.07	0.05	0.05	72.37	0.09
Tb_ppb	12	0.004	0.12	0.12	0.04	0.03	0.03	84.75	0.03
Te_ppb	12	0.000	2.71	2.71	0.53	0.27	0.78	148.15	0.79
Th_ppb	12	0.000	0.76	0.76	0.21	0.17	0.23	107.28	0.27
Ti_ppb	12	0.000	267.57	267.57	77.44	56.46	76.68	99.02	105.98
Tl_ppb	12	0.066	0.80	0.73	0.22	0.15	0.20	93.76	0.12
Tm_ppb	12	0.000	0.06	0.06	0.03	0.03	0.01	49.39	0.01
U_ppb	12	0.056	1.54	1.48	0.31	0.13	0.41	135.62	0.30
V_ppb	12	0.000	297.82	297.82	86.60	79.13	76.76	88.64	77.42
W_ppb	12	2.451	29.97	27.52	6.92	3.98	7.96	114.99	2.76
Y_ppb	12	0.184	3.46	3.27	1.04	0.67	0.99	95.76	1.42
Yb_ppb	12	0.113	0.59	0.47	0.32	0.30	0.12	35.95	0.14
Zn_ppb	12	393.297	2738.14	2344.84	855.64	567.94	688.88	80.51	555.41
Zr_ppb	12	0.000	22.43	22.43	7.22	4.20	6.84	94.71	11.08

A comparison of sap compositions from adjacent spruce and pine trees at 5 sample stations indicates similar concentrations of some elements, but consistent differences in others. These data are shown in Table A3 (Appendix 2). For most elements there is no consistency in the differences, but concentrations are similar in the sample pairs of spruce adjacent to pine. The exceptions are that in spruce, concentrations of Ba, Cd, Hg, Li, Sr and Tl are consistently higher than pine. Conversely, Cu, Fe and In are higher in the pine. Zinc is similar in both species.

Comparison between spruce sap and other organic media

It was noted earlier that a regional biogeochemical survey of the Nechako area was conducted in the 1990s, and the area encompassing Endako was completed in 1998 and 1999. That survey involved the analysis of ashed outer bark from lodgepole pine trees. Of note is that the survey was conducted prior to devastation by the pine beetle and so the selection of pine sap for comparison at all sample stations was not an option. Within the same survey area as the present study, bark samples were collected from 109 sample stations (Fig. 5). Data are presented in Appendix 3 (Table A4) in which elements shown in red font were determined by ICP-ES (the same modified aqua regia digestion as used for the Ah samples in this survey), and those in black were determined by Instrumental Neutron Activation Analysis (INAA) at Actlabs. This historical information, together with the results from Ah horizon sampling presented above, provide useful comparative datasets to test the effectiveness of spruce sap as a sample medium.

These data provide another layer of comparison of broad geochemical patterns for the area. No samples were collected from within the mine boundaries. Comparative results for Mo, La, W, Th and U are presented in Figures 18 to 22. The following plots demonstrate:

1. Molybdenum in Ah horizon, spruce sap and lodgepole pine bark show broadly similar patterns (Fig. 18). Ah horizon shows the most definitive anomaly and best contrast. Spruce sap was next best, with the pine bark appearing more diffuse, but this could be due to the lower density of pine bark samples.

2. Lanthanum (representative of the REE) exhibits broad but erratic patterns of relative enrichments within the general vicinity of the mine (Fig. 19) in all three sample media, but the clearest signature is in the spruce sap. In the Ah soils La concentrations are almost as high in samples from sites underlain by Skeena Group rocks (especially near to the contact with rocks of the Hazelton Group to the south).

3. Tungsten in spruce sap (Fig. 20) has some elevated concentrations at Endako, but there are also higher levels elsewhere in the survey area. By contrast, W in pine bark defines the mine area well. In the Ah horizon the contrast is stronger, and the anomaly more confined to the Endako mineralization.

4. Uranium in spruce sap shows a very similar pattern to W in Ah soils, but no definitive anomaly in the Ah horizon or pine bark (Fig 21).

5. Thorium in sap shows a very similar pattern to U (Fig 22), but as for U, no definitive anomaly in the Ah horizon or pine bark

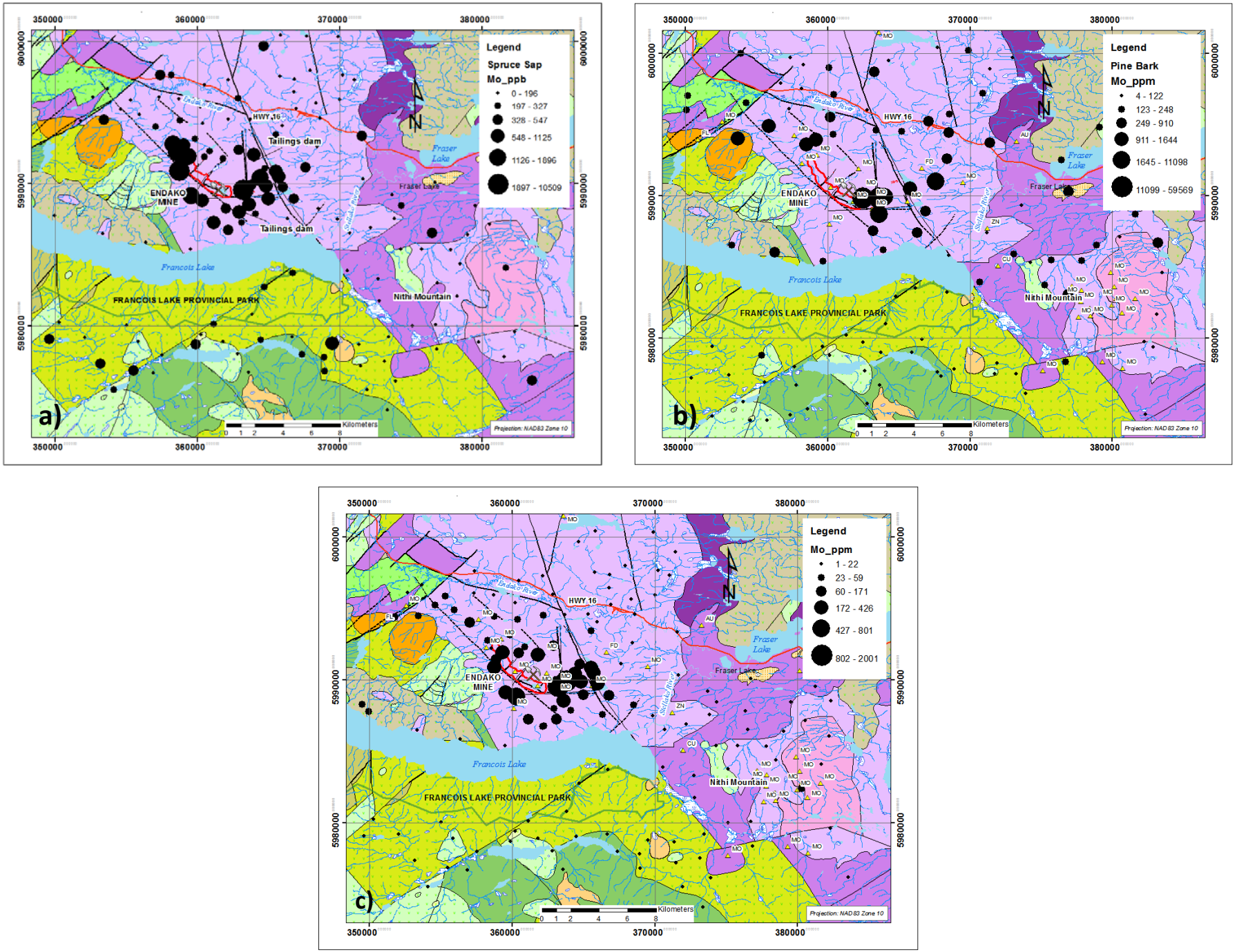

Figure 18. Molybdenum in spruce sap (a), pine bark (b) and Ah horizon (c).

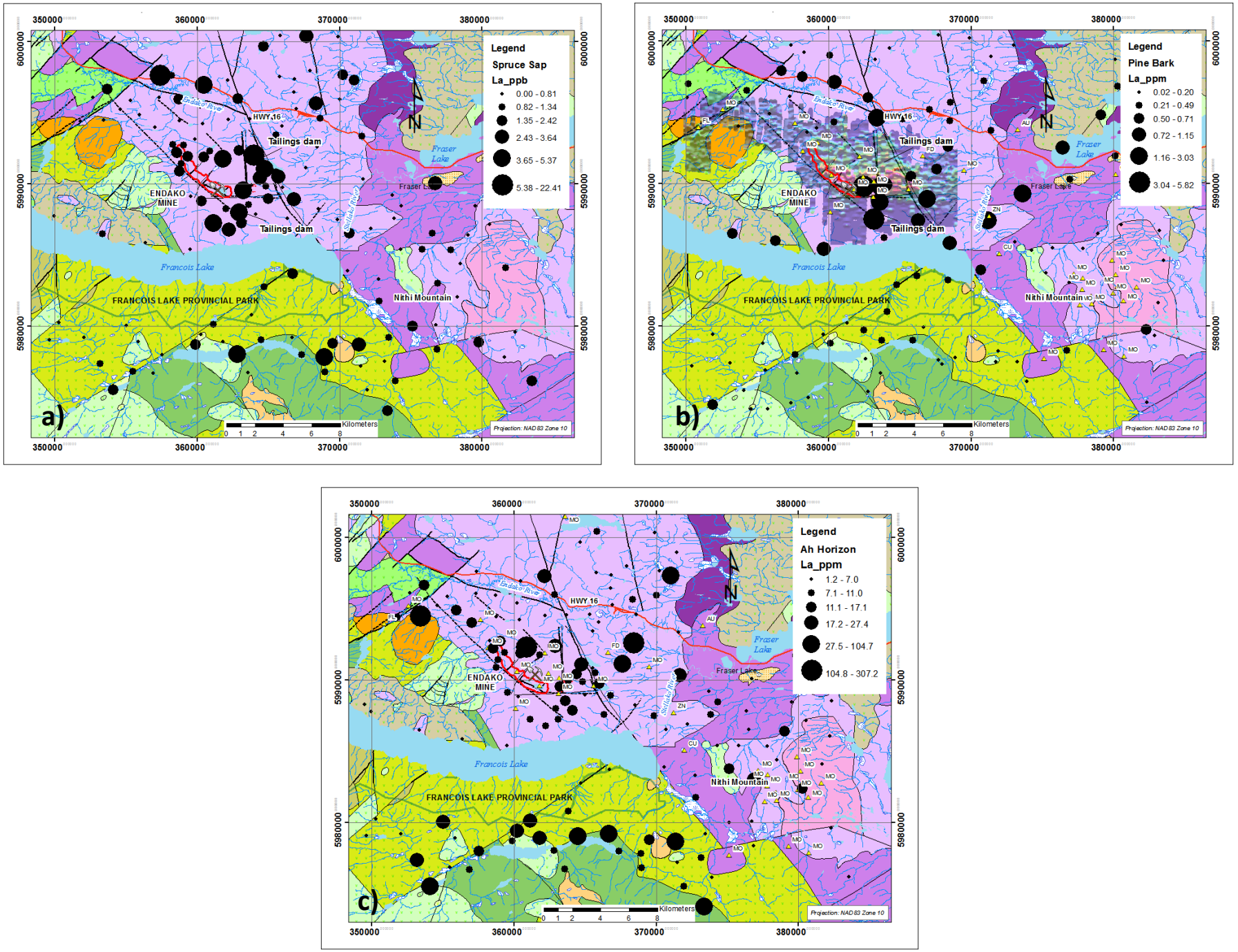

Figure 19. Lanthanum in spruce sap (a), pine bark (b) and Ah horizon (c).

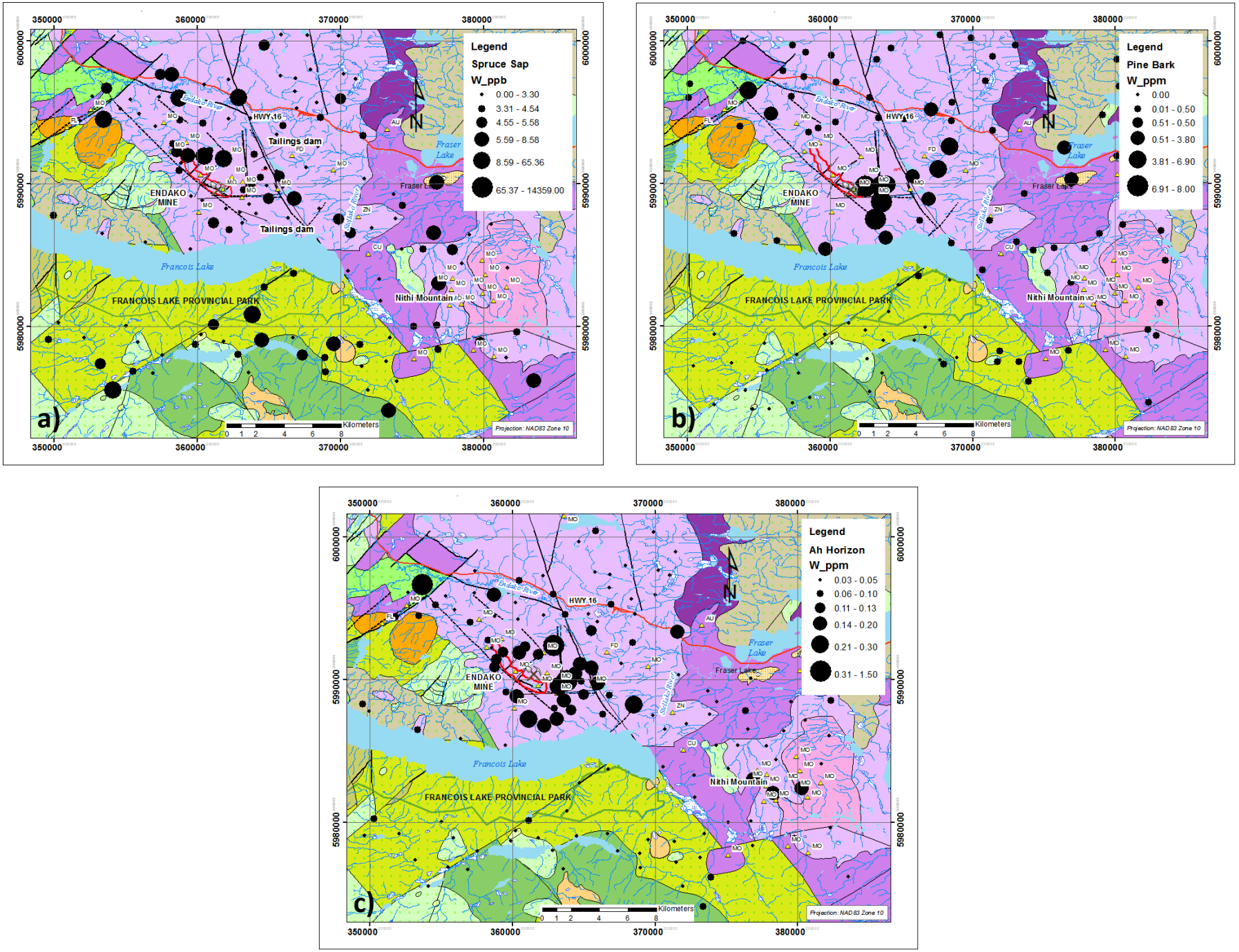

Figure 20. Tungsten in spruce sap (a), pine bark (b) and Ah horizon (c).

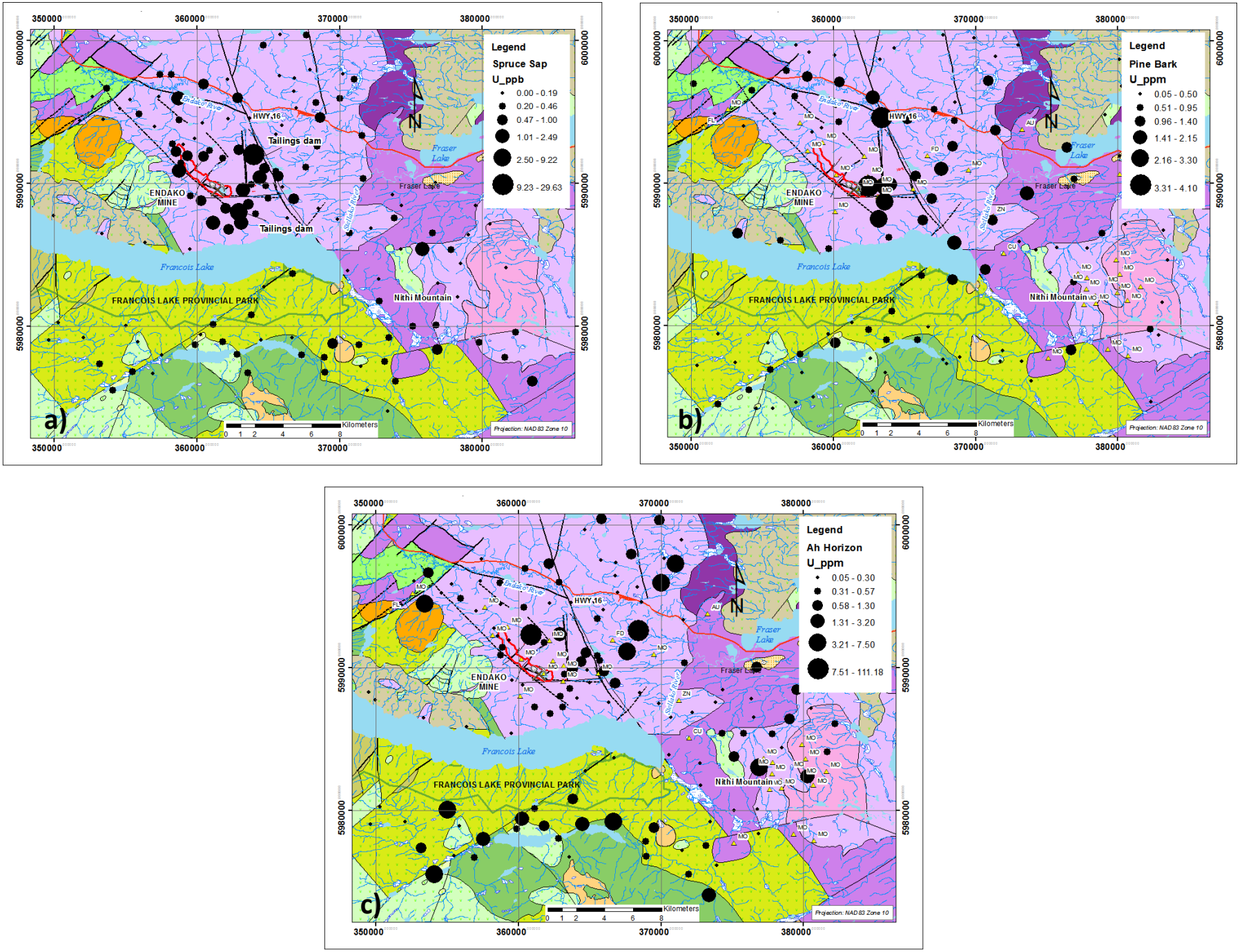

Figure 21. Uranium in spruce sap (a), pine bark (b) and Ah horizon (c).

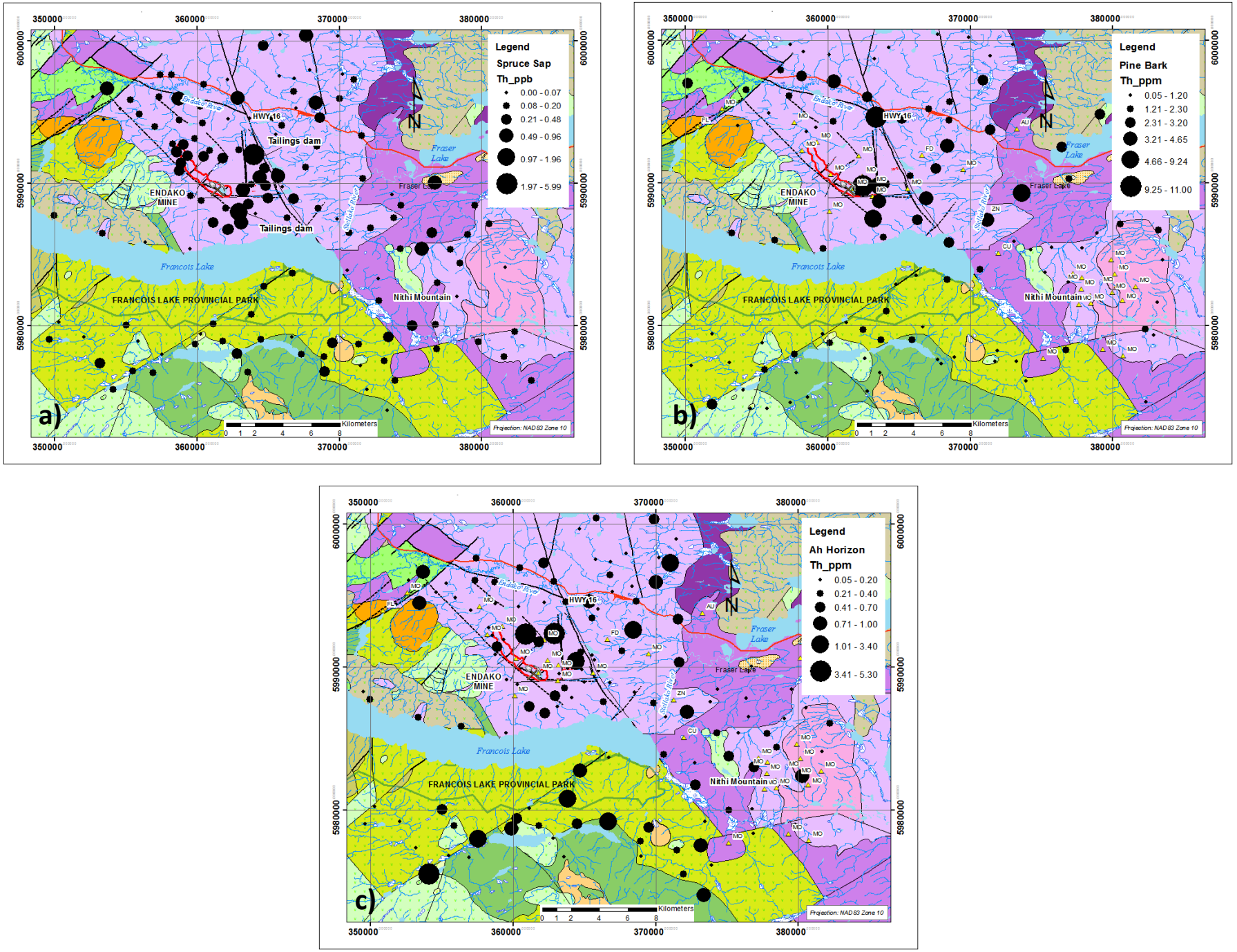

Figure 22. Thorium in spruce sap (a), pine bark (b) and Ah horizon (c).

SUMMARY CONCLUSIONS AND RECOMMENDATIONS

This project set out to establish a number of objectives concerning the use of sap samples in the exploration for mineral deposits. These are addressed in the same order as outlined at the beginning.

1. *Does sap provide information of value to mineral exploration in glaciated terrains?*

   In the environment of the Endako Mo mine there is a strong multi-element signature apparent from the analysis of small spruce sap samples. Of note are the strong signatures obtained for Mo, Re, REE, U and Th that encompass the known extent of mineralization. Positive, but less definitive signatures are shown by Ag, Bi, and to a lesser degree by Mn and Cs. Negative anomalies over the mineralized area are shown by Na, K, Rb and P. Strontium has slightly elevated levels at Endako, but this is somewhat swamped by signatures of similar magnitude to the south that appear more controlled by lithology.

2. *Can saps be used as a reliable sample medium in contaminated near-mine environments?*

   The strong signatures in the saps are from samples collected soon after they had exuded from the trees, and are not the result of a long period during which surface contaminants could have accumulated. The time period of exposure to contaminants is a factor that lends doubt to signatures found in other surface media, such as Ah soils and outer bark of conifers. Furthermore the sample preparation and digestion procedure used (see point 4 below) was designed to filter out any mineral dust contamination that may be adhered to or included in the sap.

3. *What are the recommended sampling strategies for the collection of saps?*

   Sap accumulates mostly as clean discrete globules of amber to yellow resinous material that can be picked off the surface with the point of a penknife. The small bark particles that readily fall off the tree with the sap can be removed by gently blowing into the container used for collection (frontispiece). Each sample took only a few minutes to collect ~2 g into a glass vial.

4. *What is the optimal sample preparation and analytical procedure to be employed for obtaining precise data?*

   This aspect of the study was left to the analytical laboratory (Actlabs) to determine. After experimentation with a number of different organic solvents and acids, and varying dilutions it was determined that the optimal method involved first cleaning the sap by dissolving it in methanol and passing the solution through a 0.45 µm filter. The filtered sap solution was then allowed to re-solidify and a 0.25 g aliquot of the pure sap was digested in nitric-perchloric acid and analyzed by high sensitivity ICP-MS.

5. *What levels of detection are required to see the geochemical signatures of saps?*

   For most elements detection levels need to be at sub-ppb levels, including Ag, Au, Be, most of the REE, Hf, In, Nb, Pd, Pt, Ta, Te, Th, Tl, U and Y in order to determine spatial variations. At these low levels, analytical precision is poor and so data need to be carefully screened before attempting to plot values, otherwise false conclusions could be made. A further complication is the rather poor

reproducibility of some elements in field duplicates – even those with concentrations well above the detection limit such as the major elements and most base metals.

6. *How does the geochemical signature of sap compare to signatures from those of organic-rich soils (Ah horizon) and of bark tissues (data obtained from previous surveys), and is the signature from saps more definitive for delineating known mineralization than in the other media?*

   Comparisons are made with data obtained from Ah horizon samples collected at the same sample stations as the saps and the same time, and from a regional survey conducted in the 1990s involving the collection and analysis of pine bark, but at lower sample density. The distribution patterns of Mo showed that Ah horizon provided the best definition of the Endako anomaly but spruce sap was quite comparable and also produced a robust response that was more clearly defined than the pine bark patterns. For the REE, spruce sap outperformed the other media and produced a high contrast anomaly at the east end of the Endako deposit. This result confirms REE patterns identified by the original 1990s pine bark survey. Ah horizon REE results did not convincingly highlight the Endako area but did produce an important response over the Skeena Group on the south side of François Lake. There was no W response in spruce sap at Endako despite strong W patterns in Ah horizon and pine bark. For U and Th, spruce sap produced convincing responses around Endako that were not visible in the pine bark or Ah horizon results. As might be expected, the sap and Ah samples that were collected at the same time (identical locations) had more similarities than with the lower density pine bark samples from the same general area.

7. *Do saps from pines provide similar information, and can the data from different species be integrated or do they need to be levelled for comparison?*

   Because of pine beetle kill over the past decade, there were only a few sample stations where both pine and spruce were present in order to make this comparison. Furthermore, it was found that many pines had little or no sap on their bark surfaces, since they tend to have minute traces of sap scattered over the bark surface and are quite impractical to collect. The 5 sites compared showed inconsistent patterns and there was insufficient information to be able to determine if data from the two species could be levelled and then integrated. All that could be established was that for the majority of elements spruce sap tends to be relatively enriched with respect to pine, but pine sap tends to have higher concentrations in Al, Be, Cd, Cu, Fe, Mg, P and Sb than spruce sap.

ACKNOWLEDGEMENTS

The authors wish to thank Geoscience BC for their support for this project. We thank Michael Pond from Endako for his help and guidance during the second sampling campaign within the mine fence, and Thompson Creek Metals Company Inc. for permission to enter the mine site. Thanks also to Ray Lett, Peter Bradshaw, Bruce Madu and Christa Pellett for reviewing this manuscript and for their helpful and insightful comments.

REFERENCES

Abzalov, M.Z. (2008). Quality Control of Assay Data: A Review of Procedures for Measuring and Monitoring Precision and Accuracy, Exploration and Mining Geology, 17(3-4): 1-14.

Bissig, T., Heberlein, D.R. and Dunn, C, E. (2013): Geochemical Techniques for Detection of Blind Porphyry Copper-Gold Mineralization under Basalt Cover, Woodjam Property, South-Central British Columbia (NTS 093A/03, /06): Geoscience BC Report 2013-17, 54 p.

British Columbia Ministry of Forests (1988). Biogeoclimatic Zones of British Columbia, 2014. Province of British Columbia, Ministry of Forests, Research Branch, Victoria, BC (1 map).

Devine, F.A.M., Pond, P., Heberlein, D.R., Kowalczyk, P., Kilby, W. and Ma, F. (in press). A geo-exploration atlas of the Endako porphyry molybdenum district; Geoscience BC, 43 pp.

Dunn, C.E. (1998). Regional and detailed biogeochemical surveys in the Nechako NATMAP area and in the Babine Porphyry Belt, in: New Geological Constraints on Mesozoic to Tertiary Metallogenesis and on Mineral Exploration in Central British Columbia: Nechako NATMAP Project, L.C. Struik and D.G. MacIntyre, eds. Short Course Extended Abstracts, Cordilleran Section of the Geological Association of Canada (March 27): 17 pp.

Dunn, C.E. (2007). Biogeochemistry in Mineral Exploration; *in* Handbook of Exploration and Environmental Geochemistry, Volume 9, M. Hale (ed.), Elsevier, Amsterdam, 464pp.

Dunn, C.E., and Hastings, N.L. (1998a). Biogeochemical survey of the Ootsa-Francois Lakes area using outer bark of lodgepole pine (NTS 93F 13/14 and part of 12 - North-Central British Columbia): Base Metals and Pathfinder Elements. Geological Survey of Canada, Open File 3587a. 1 sheet of coloured maps.

Dunn, C.E., and Hastings, N.L. (1998b). Biogeochemical survey of the Ootsa-Francois Lakes area using outer bark of lodgepole pine (NTS 93F 13/14 and part of 12 - North-Central British Columbia): Mafic Suite of Elements with Thorium and Lanthanum. Geological Survey of Canada, Open File 3587b. 1 sheet of coloured maps.

Dunn, C.E., and Hastings, N.L. (1998c). Biogeochemical survey of the Ootsa-Francois Lakes area using outer bark of lodgepole pine (NTS 93F 13/14 and part of 12 - North-Central British Columbia): Alkali Metals, Alkaline Earths, Manganese and Aluminum. Geological Survey of Canada, Open File 3587a. 1 sheet of coloured maps.

Dunn, C.E., and Hastings, N.L. (1998d). Biogeochemical survey of the Ootsa-Francois Lakes area using outer bark of lodgepole pine (NTS 93F 13/14 and part of 12 - North-Central British Columbia): Digital Data Listings and Summary Notes. Geological Survey of Canada, Open File D3587d.

Dunn, C.E. and Hastings, N.L. (1999a). Biogeochemical survey of the Fraser Lake area using outer bark of lodgepole pine (NTS 93K/2 and 93K/3): Base Metals, Gold and Pathfinder Elements. Geological Survey of Canada, Open File 3696a. 1 sheet of coloured maps.

Dunn, C.E. and Hastings, N.L. (1999b). Biogeochemical survey of the Fraser Lake area using outer bark of lodgepole pine (NTS 93K/2 and 93K/3): Mafic Suite of Elements with Thorium and Lanthanum. Geological Survey of Canada, Open File 3696b. 1 sheet of coloured maps.

Dunn, C.E. and Hastings, N.L. (1999c). Biogeochemical survey of the Fraser Lake area using outer bark of lodgepole pine (NTS 93K/2 and 93K/3): Alkali Metals, Alkaline Earths, Manganese and Aluminum. Geological Survey of Canada, Open File 3696c. 1 sheet of coloured maps.

Dunn, C.E. and Hastings, N.L. (1999d). Biogeochemical survey of the Fraser Lake area using outer bark of lodgepole pine (NTS 93K/2 and 93K/3): Digital Data Listings and Summary Notes. Geological Survey of Canada, Open File D3696d.

Ferbey, T., Arnold, H., Hickin, A.S. (2013). Ice-flow indicator compilation, British Columbia, BCGS Open File, 2013-06.

Hamilton S.M., Cameron E.M., McClenaghan M.B., Hall G.E.M. (2004a). Redox, pH and SP variation over mineralization in thick glacial overburden, Part I. Methodologies and field investigation at the Marsh zone gold property. Geochemistry: Exploration, Environment, Analysis, 4, 33–44.

Hamilton S.M., Cameron E.M., McClenaghan M.B., Hall G.E.M. (2004b). Redox, pH and SP variation over mineralization in thick glacial overburden, Part II. Field investigation at Cross lake VMS property. Geochemistry: Exploration, Environment, Analysis, 4, 45–58.

Harju, L. and Huldén, S.G. (1990). Birch sap as a tool for biogeochemical prospecting; Journal of Geochemical Exploration, v.37, p.351–365.

Heberlein, D.R., Dunn, C.E. and MacFarlane, W. (2013). Use of Organic Media in the Geochemical Detection of Blind Porphyry Copper-Gold Mineralization in the Woodjam Property Area, south-central BC (NTS 093A/03, /06). Geoscience BC Report 2013-20, 86 pp. + appendices.

Holland, S.S. (1976). Landforms of British Columbia: a physiographic outline. 2nd ed. B.C. Dep. Mines Pet. Resources, Bull. No. 48. Victoria, B.C.

Krendelev, F.P. and Pogrebnyak, Y. F. (1979). Gold and Zinc concentrations in birch sap as prospecting indicators for these metals; Doklady Akademii Nauk SSSR 234, p. 250–252.

Kyuregyan, E. A. and Burnutyan, R.A. (1972). Gold in the juice of plants as a method for its detection (in Russian); Izd-vo Akademii Nauk Ar. SSSR 25, p. 83–85.

Mosher, G.Z. (2011). Technical report on the Nithi Mountain Molybdenum property, British Columbia, Canada. NI 43-101 technical report for Leeward Capital Corp., 50 pp.

Plouffe, A. (2007). Surficial geology (93F, K and N) for the Nechako NATMAP Project in Nechako NATMAP Project: A digital suite of geoscience information for central British Columbia; Geological Survey of Canada, Open File 5623 and British Columbia Ministry of Energy, Mines and Petroleum Resources, Open File 2007-10.

Selby, D. and Creaser, R.A. (2001). Re-Os Geochronology and Systematica in Molybdenite from the Endako Porphyry Molybdenum Deposit, British Columbia, Canada; Economic Geology, vol. 96, p. 197-204.

Smee B.W. (1983). Laboratory and field evidence in support of the electrochemically-enhanced migration of ions through glaciolacustrine sediment. Journal of Geochemical Exploration, 19, 277–304.

Stanley, C.R., Smee, B.W. (2007). Strategies for reducing sampling errors in exploration and resource definition drilling programs for gold deposits. Geochemistry: Exploration, Environment, Analysis, Vol. 7, No. 4, 329-340.

Villeneuve, M., Whalen, J.B., Anderson, R.G. and Struik, L. C., (2001). The Endako Batholith: Episodic plutonism culminating in formation of Endako porphyry molybdenite deposit, North-Central British Columbia; Economic Geology, vol. 96, p. 171-196.

Warren, H.V. and Delavault, R.E. (1965). Further studies of the biogeochemistry of molybdenum; Western Miner, October: 5 pp.

Warren, H.V. and Horsky, S.J., (1982). Further notes on the use of pollen as an exploration tool; Western Miner, May, 42-44.

Warren, H.V., Delavault, R.E., and Routley, D.G. (1953). Preliminary studies of the biogeochemistry of molybdenum, Transactions of the Royal Society of Canada, Series 3, 47, Section 4: 71-75.